COMPONENT PART NOTICE

THIS PAPER IS A COMPONENT PART OF THE FOLLOWING COMPILATION REPORT:

TITLE: Hypersonic Combined Cycle Propulsion Panel Symposium (75th) Held in Madrid, Spain on 28 May - 1 June 1990 (La Propulsion Hypersonique a Cycles Combines.

TO ORDER THE COMPLETE COMPILATION REPORT, USE AD-A253 867.

THE COMPONENT PART IS PROVIDED HERE TO ALLOW USERS ACCESS TO INDIVIDUALLY AUTHORED SECTIONS OF PROCEEDING, ANNALS, SYMPOSIA, ETC. HOWEVER, THE COMPONENT SHOULD BE CONSIDERED WITHIN THE CONTEXT OF THE OVERALL COMPILATION REPORT AND NOT AS A STAND-ALONE TECHNICAL REPORT.

THE FOLLOWING COMPONENT PART NUMBERS COMPRISE THE COMPILATION REPORT:

AD#: AD-P007 938	AD#: AD-P007 965
AD#:	AD#:
AD#:	AD#:

TURBOJET POTENTIAL FOR HYPERSONIC FLIGHT

by
Jeffrey M. Stricker & Douglas J. Essman
Turbine Engine Division
Wright Research & Development Center (WRDC/POTA)
Wright-Patterson Air Force Base, Ohio USA 45433

INTRODUCTION

Over the past few years, interest in manned hypersonic flight has increased significantly. System studies historically have utilized ramjet power for high supersonic/low hypersonic speeds and supersonic combustion ramjets (scramjets) at higher speeds. The drawback of these types of propulsion devices is their inability to perform at takeoff and relatively low speeds. Therefore, for relatively low speed operation (Mach 0-3), a third form of propulsion is required. The turbine engine has typically been chosen for this role.

The disadvantages of a three mode propulsion system (turbojet-ramjet-scramjet) are the complexity, weight and costs which accompany it. Inlet and exhaust geometry variations required for proper integration play a major role. Propulsion weight is a key factor to maximize vehicle capability. When a propulsion device is not being utilized, it is dead weight to the aircraft system. Therefore, for reasons of simplicity, reduced system weight, and cost, it seems prudent to minimize the number of propulsion mode transitions required.

This paper will explore the utilization of the turbine engine for aircraft propulsion up to the scramjet transition. Examination of the uninstalled cycle performance is presented as well as an assessment of installed engine operation in a hydrogen fueled aircraft. Both non-afterburning and afterburning (A/B) turbine engines are compared to turboramjet and air-turboramjet (ATR) engines for a Mach 5 long duration cruise mission along with a pure acceleration mission, i.e., the turbomachinery is used to accelerate the vehicle to a Mach number where the scramjet can take over. From this assessment, a baseline engine configuration/cycle is defined for feasibility studies and critical technology identification. A discussion of the feasibility of the preferred concept from an engine component by component standpoint is provided as well as a discussion of technology risk compared to the state-of-the-art.

UNINSTALLED PERFORMANCE

To determine the desirability of turbomachinery at hypersonic velocities, it is useful to ascertain whether the turbine engine provides competitive uninstalled performance compared to devices more commonly considered for hypersonic flight. Four types of turbopropulsion devices were studied; a cooled non-afterburning (dry) turbojet, an uncooled afterburning (A/B) turbojet, a turboramjet, and an uncooled recuperated air-turboramjet (ATR) (Figure 1). In all cases, hydrogen was used for fuel. For turbomachinery operating above Mach 4, a fuel-air heat exchanger was used for cooling compressor bleed air. Fuel inlet temperature to the heat exchanger was assumed to be 800°F, simulating fuel usage for vehicle cooling. The turbine inlet temperature of the ATR was limited to 2050°F due to heat exchanger, fuel delivery and uncooled expander turbine material limitations. Maximum burner temperature was limited to stoichiometric combustion. Table 1 shows a comparison of the various cycles.

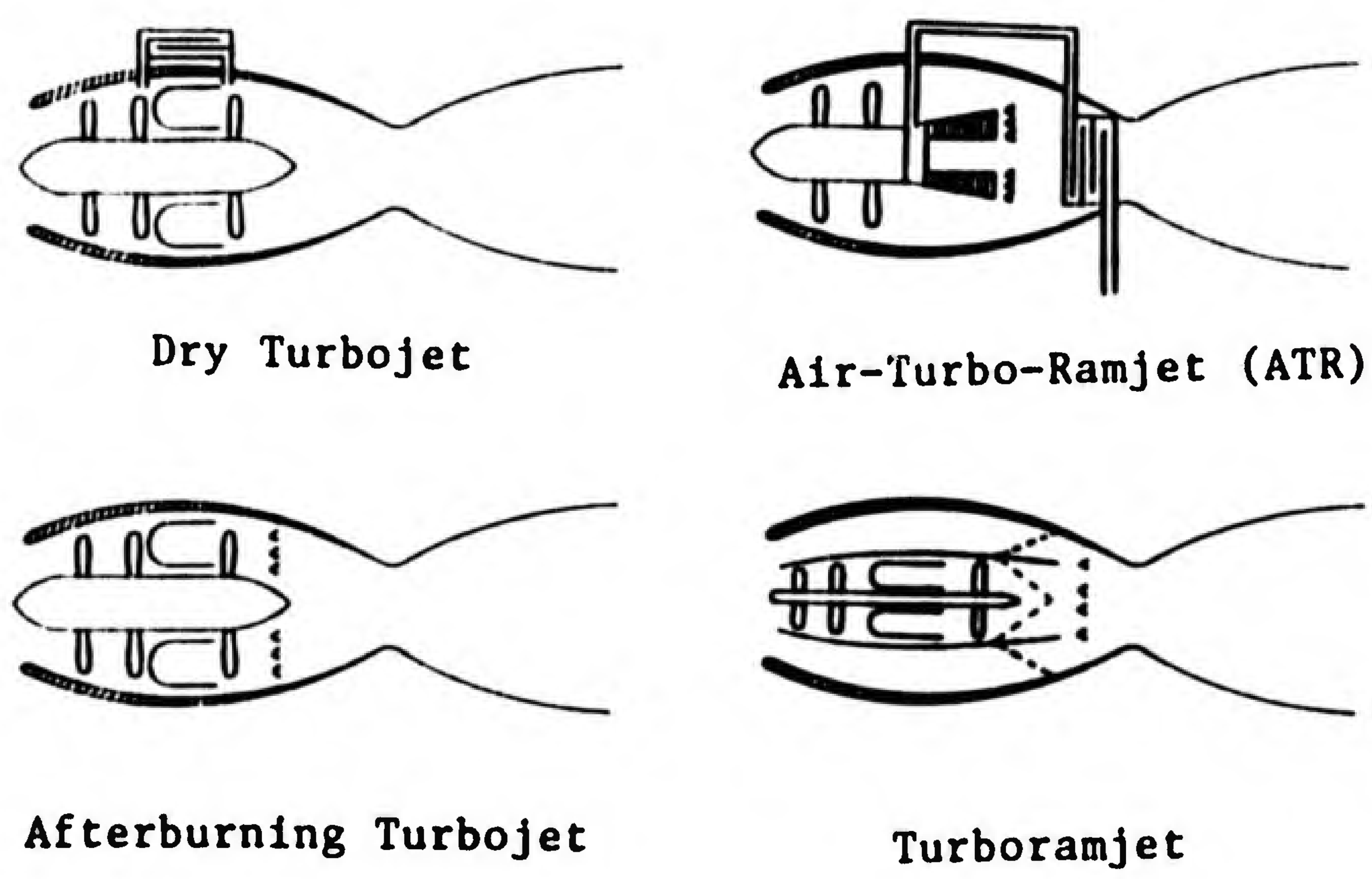

Figure 1 - Cycles Examined

Figure 2 illustrates the performance of the cooled non-A/B turbojet, uncooled A/B turbojet, turboramjet, and ATR operating between Mach 5 and 6. Even with extremely high turbine temperature capability, the dry turbojet exhibits poor specific thrust performance relative to the other forms of propulsion. The afterburning turbine engine utilizing a more conservative turbine rotor inlet temperature (TRIT = 2800°F) is very competitive with the turboramjet and ATR in thrust performance and advantageous from a fuel consumption standpoint. The competitive performance of the ATR is primarily due to the higher nozzle pressure ratio which may not be useful in an actual application due to nozzle size limitations (Figure 2 assumes full expansion of exhaust gasses). In all cases, performance degrades rapidly as Mach number is increased.

It is envisioned that the weapon system transitions to the scramjet propulsion mode at a Mach number between 5 and 5.5. This is primarily because of performance degradation and material constraints for the turbomachinery as well as minimum Mach number capability for the scramjet. Component design sensitivities to performance for the dry turbojet were evaluated to determine the criticality of the design parameters (Figure 3). The most vital parameters to performance were burner efficiency and exhaust nozzle performance (CFG). The latter was found to be the most critical with a 3.8 percent reduction in net specific thrust for each percent loss in thrust coefficient. Rotating component efficiencies were found to be less critical. The baseline leakage was .5%. This small level of leakage tends to make percentage changes in leakage appear

	A/B TJ	DRY TJ	TURBORAMJET	ATR
Pressure Ratio	10	10	10	5
Throttle Ratio (T4max/T4)	1.114	1.114	1.114	---
Main Burner Temp.	2800°F	4000°F	4000°F	---
Afterburner/Ramburner Temp.	Stoich	---	Stoich	Stoich
Efficiencies:				
Compressor	85%	85&	85%	85%
Main Burner	99%	99%	99%	99%
Turbine	85%	85%	85%	70%
Afterburner/Ramburner	95%	---	90%	---
Cooling:				
Turbine Stator	0.0%	5.5%[1]	5.5%[1]	0.0%
Turbine Rotor	0.0%	6.0%[2]	6.0%[2]	0.0%
Exhaust Nozzle	15%[3]	10%[3]	10%[3]	5%
Transition Mach Number	---	---	4-5	---
Pressure Losses:				
Main Burner	9%	9%	9%	9%
Rear Duct	1%(cold)[4]	4%	4%(cold)[4]	4%(cold)[4]
Gross Thrust Coefficient	.985	.985	.985	.985
Engine Thrust/Weight	10	10	10	10

1 - Varied to give 2800°F Tmetal
2 - Varied to give 2700°F Tmetal
3 - Compressor interstage bleed
4 - Hot loss is a function of exhaust temperature

Table 1 - Baseline Cycle Comparison (Sea Level Static)

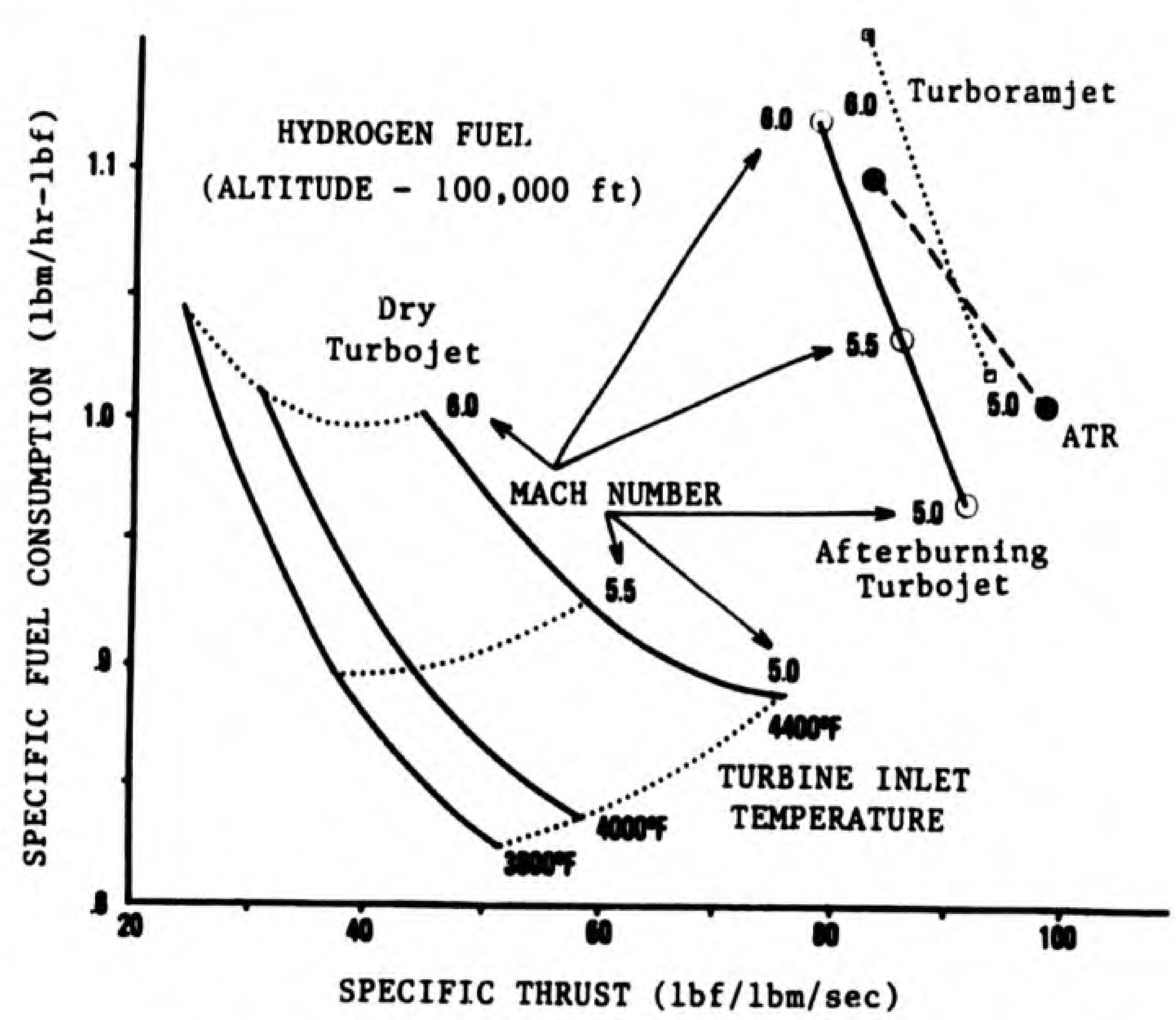

Figure 2 - Performance Comparison (Uninstalled)

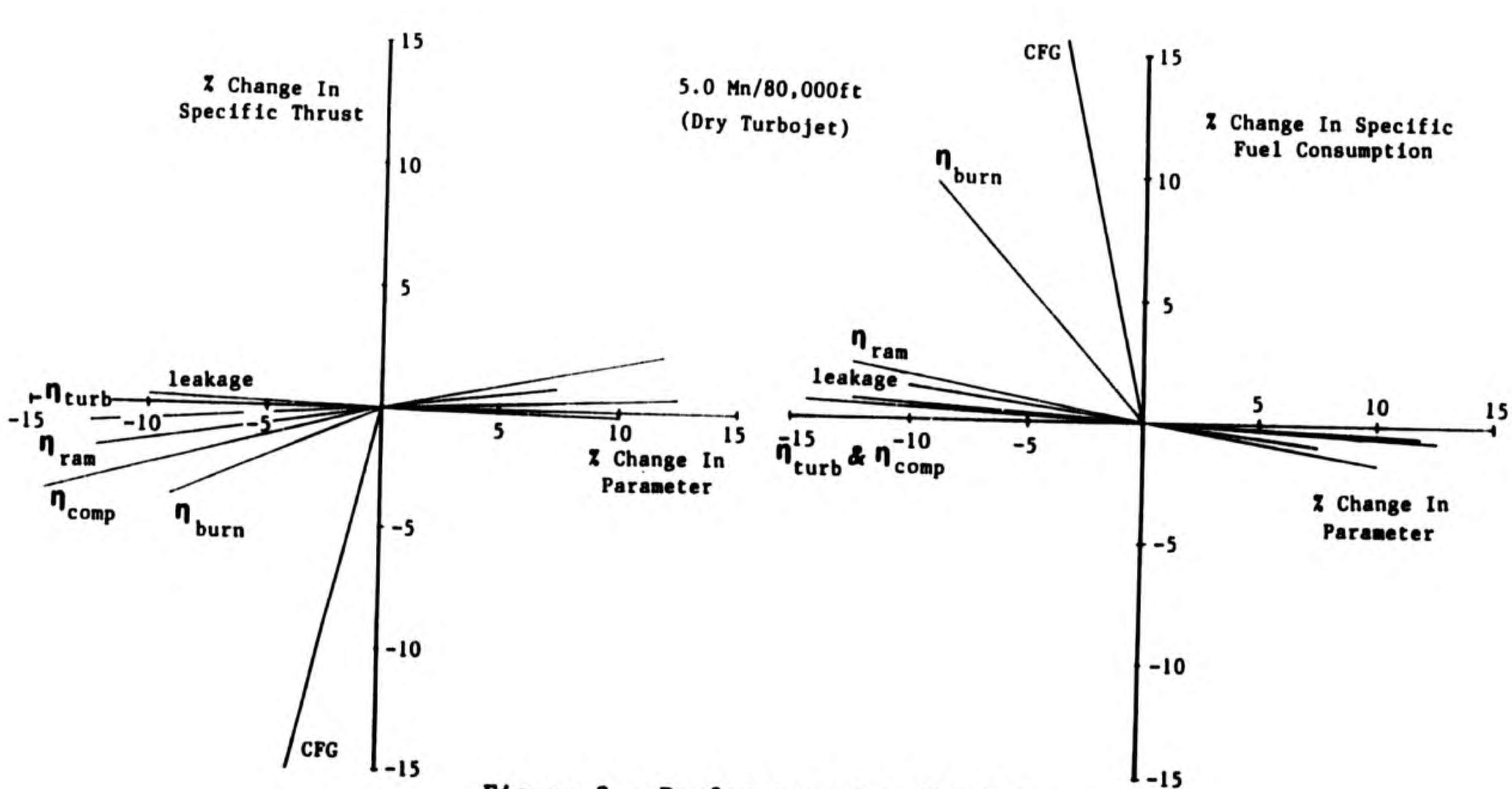

Figure 3 - Performance Sensitivity

to have a small impact on performance. In reality, leakage could increase dramatically which will have a profound impact on performance. Hence, leakage is also an important parameter to achieve good performance.

With the aid of an engine simulation model, part power performance of the various cycles was determined. Advanced compressor maps were generated and utilized for each engine. Both turbine engines were operated with a throttle ratio just over 1.1. Throttle ratio is defined as maximum combustor exit temperature over sea level static combustor exit temperature. Throttle ratio is a method to hold corrected airflow constant up to a given inlet temperature resulting in increased thrust at elevated inlet temperatures. As flight speed increases, turbine inlet temperature increases to maintain constant corrected flow. This can continue until maximum turbine inlet temperature is reached. An installed analysis to determine optimum throttle ratio was performed and will be discussed in a later section. Figure 4 illustrates that, at a given thrust level, the turbojet cycles have more favorable specific fuel consumption which potentially translates to increased range. The dry turbojet nearly equals the afterburning turbojet cruise fuel consumption, but pays a penalty in terms of reduced maximum specific thrust.

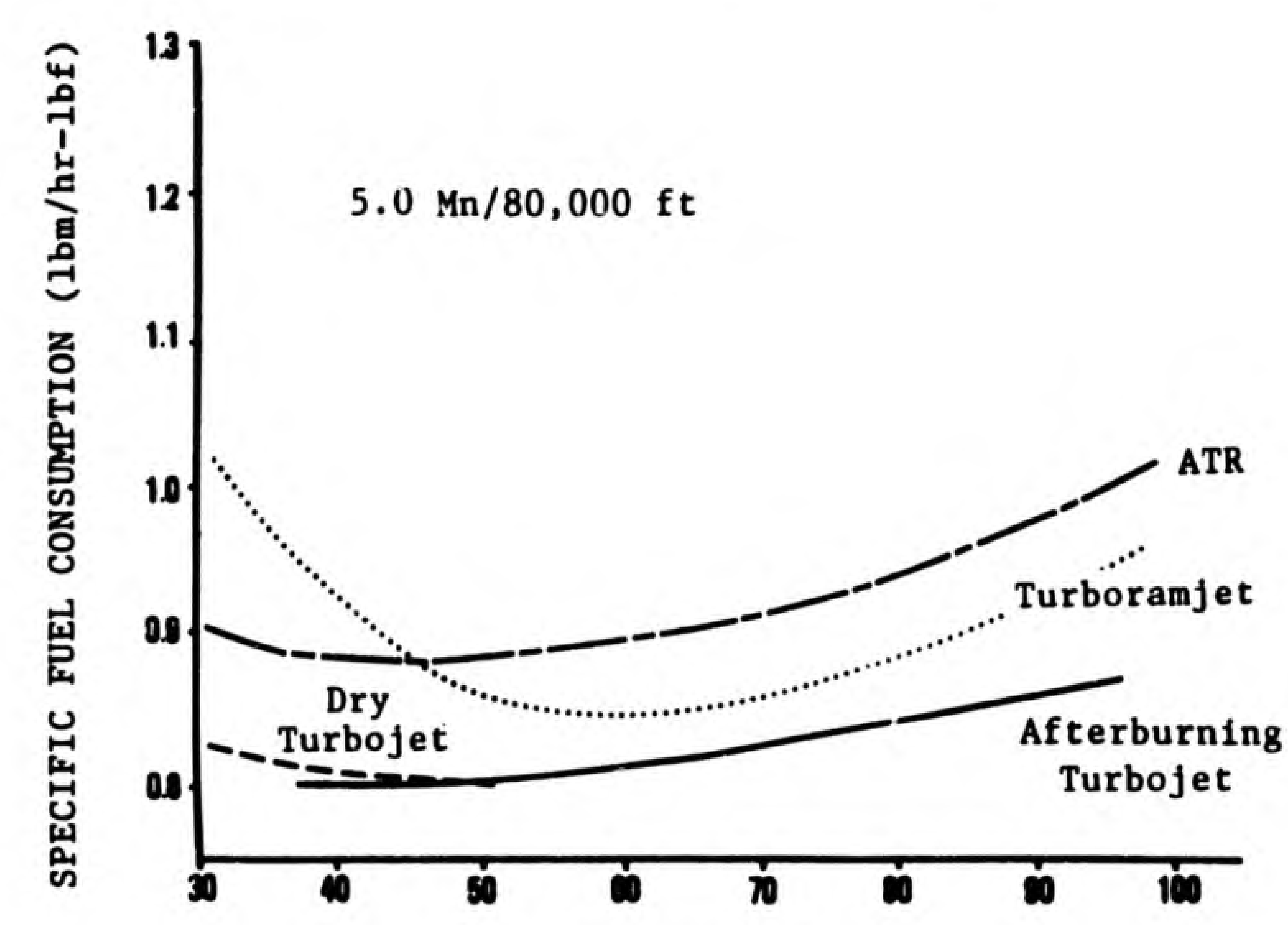

Figure 4 - Engine Cycle Power Hooks

Another key flight point occurs during acceleration through the transonic drag rise. A comparison of the various turbopropulsion system's performance is shown in Figure 5. For the turbojet cycles, increasing pressure ratio increases specific thrust and reduces specific fuel consumption. Diminishing improvements in performance for pressure ratios above 10 imply limited benefits for pressure ratios above this level. For the dry turbojet, increasing turbine inlet temperature increases specific thrust along with specific fuel consumption. For the afterburning engine, increasing turbine inlet temperature decreases specific fuel consumption accompanied by a smaller increase in specific thrust. The ATR nearly parallels the 5 pressure ratio afterburning engine in specific fuel consumption yet presents a much higher specific thrust. This is due to a much higher nozzle pressure ratio (NPR). Concluded are that both dry and afterburning turbojets should be designed for moderate SLS pressure ratios and that maximum turbine inlet temperature is critical to the dry turbojet. An installed analysis was performed to further examine desirable cycle characteristics.

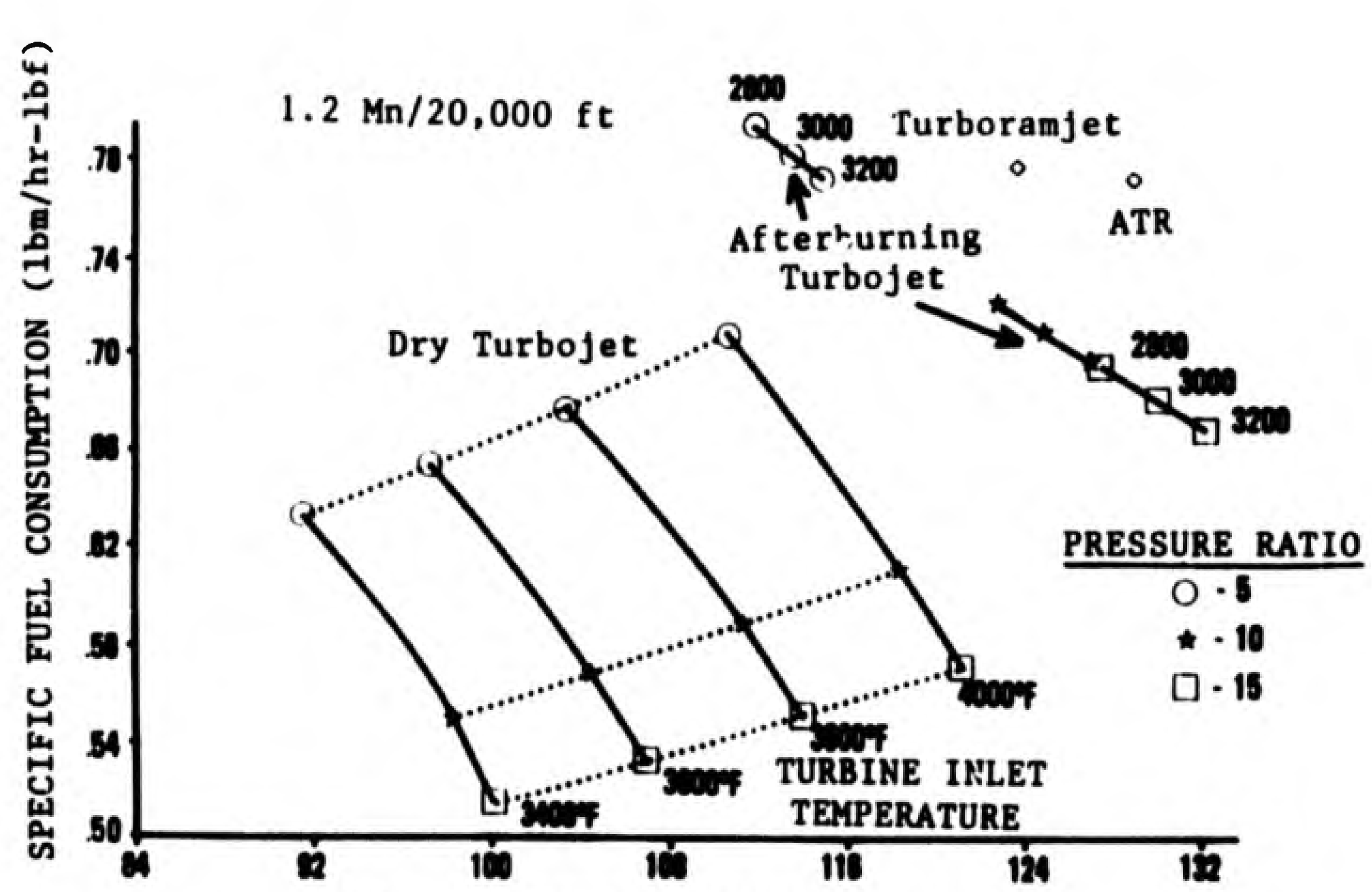

Figure 5 - Transonic Performance Comparison

From the uninstalled performance assessment, the afterburning and dry turbojet cycles are competitive with other forms of high speed propulsion devices. The afterburning turbojet offers desirable specific fuel consumption with competitive specific thrust compared to the ATR and turboramjet. The dry turbojet offers favorable specific fuel consumption characteristics, but delivers low specific thrust relative to the other cycles.

INSTALLED PERFORMANCE - LONG DURATION CRUISE VEHICLE (LDCV)

The aircraft described in Table 2 was used for turbomachinery propulsion system evaluation for a Mach 5 cruise flight mission. Figure 6 illustrates the drag polars for the vehicle. The reference area used is 1764.3 square feet.

The inlet design was derived from the NASA HYCAT-1A (Ref. 2). This vehicle was designed for Mach 6 operation. Modifications were

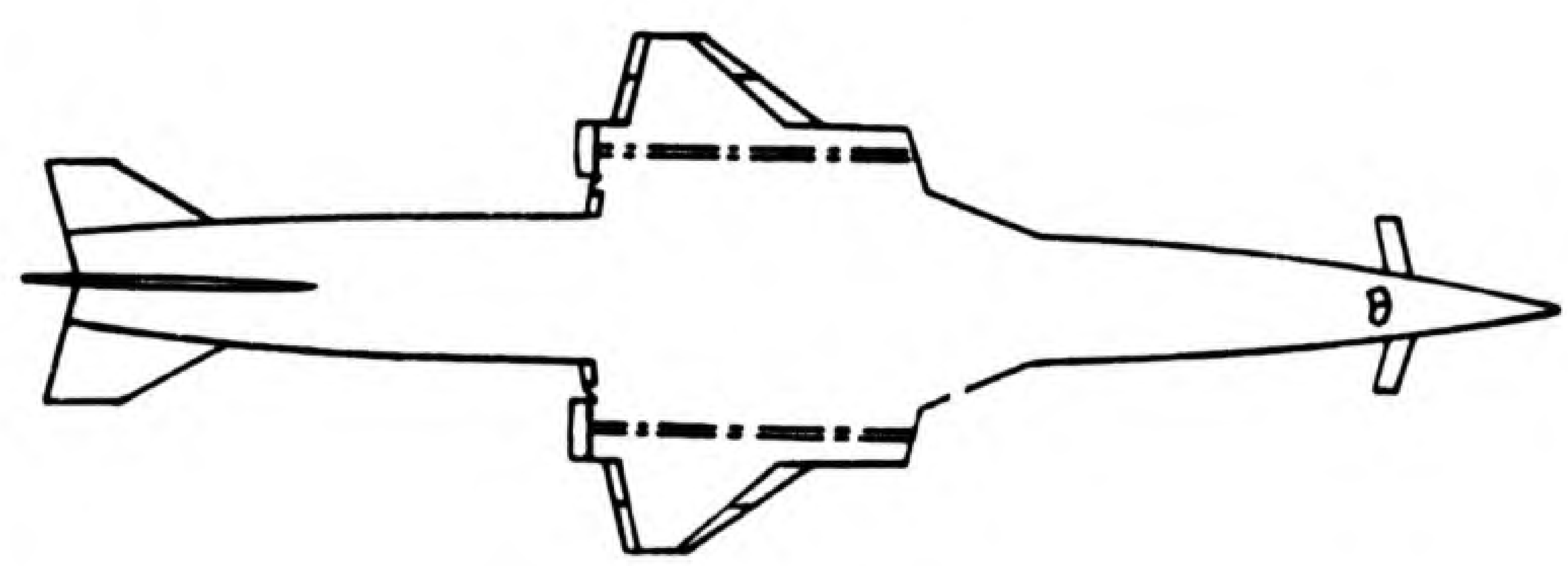

Fuel	Hydrogen
Take Off Gross Weight	140,000 Lbs
Payload	5000 Lbs
Engine Plus Fuel Fraction	45.8%
Wing Span	54.8 Ft
Wing Loading	79.3 lbs/Sq Ft
Wing Aspect Ratio	1.7
Wing Planform	Cranked Arrow
Propulsion	4 Close Coupled, Pod Mounted Engines, (2 per Nacelle)
Inlet	Mixed Compression
Nozzle	Fully Expanded C-D Axisymmetric (Referee)

TABLE 2 - AIRCRAFT CHARACTERISTICS

necessary to utilize this inlet in a Mach 5 vehicle. A delta drag coefficient, as a function of flight Mach number, was applied to the HYCAT inlet to account for the variation of critical spillage drag. The delta spillage drag coefficient was subtracted from the total inlet drag coefficient across the flight envelope in order to redesign the inlet for Mach 5 operation.

The mission assumes that the aircraft takes off and climbs at a constant flight dynamic pressure (q) of 1000 pounds per square foot (PSF) until it reaches Mach 5. It then begins a Brequet cruise radius mission with a 180 degree, 1 1/2g turn to return to base. Aircraft takeoff gross weight was held constant with radius being the figure of merit (FOM). For the installed performance assessment, all data is referenced to the baseline dry turbojet.

Evaluation of turbojet thrust sizing requirements revealed variations as a function of engine cycle. The dry turbojet is sized at the cruise condition due to its lack of hypersonic thrust performance while the afterburning engine, because of its stoichiometric augmentor, has its thrust sizing point in the transonic drag rise region.

Figure 7 shows how the turbine engines at various pressure ratios compare to the turboramjet and ATR. Inlet sizing was not optimized for the turboramjet, thereby allowing a qualitative assessment only. Maximum range for the dry turbojet occurs at higher pressure ratio designs than in the afterburning case due to balancing variations in thrust sizing and its effects on the amount of power throttling required at cruise. Both the dry and afterburning engines appear competitive to the ATR and turboramjet.

Figures 8 and 9 illustrate mission performance variations to key engine operating characteristics. High throttle ratio designs are attractive to the dry engine configuration since this increases the flow size of the engine transonically for better inlet matching and provides higher thrust for high Mach flight conditions. The afterburning engine with its inherently higher specific thrust optimizes at a lower throttle ratio for enhanced fuel management. Increasing the turbine temperature of the dry turbojet shifts the optimum pressure

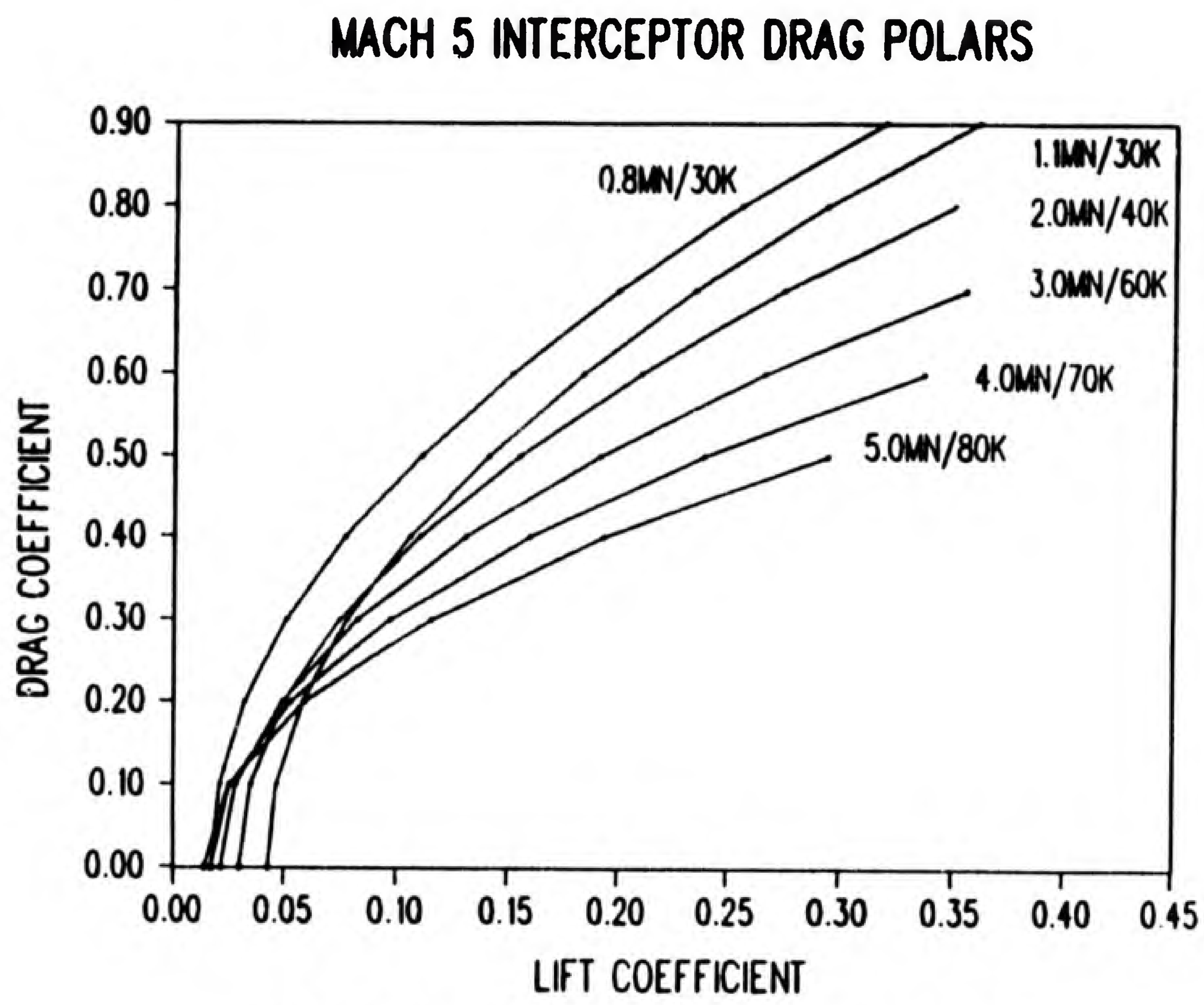

Figure 6 - Mach 5 Interceptor Drag Polar

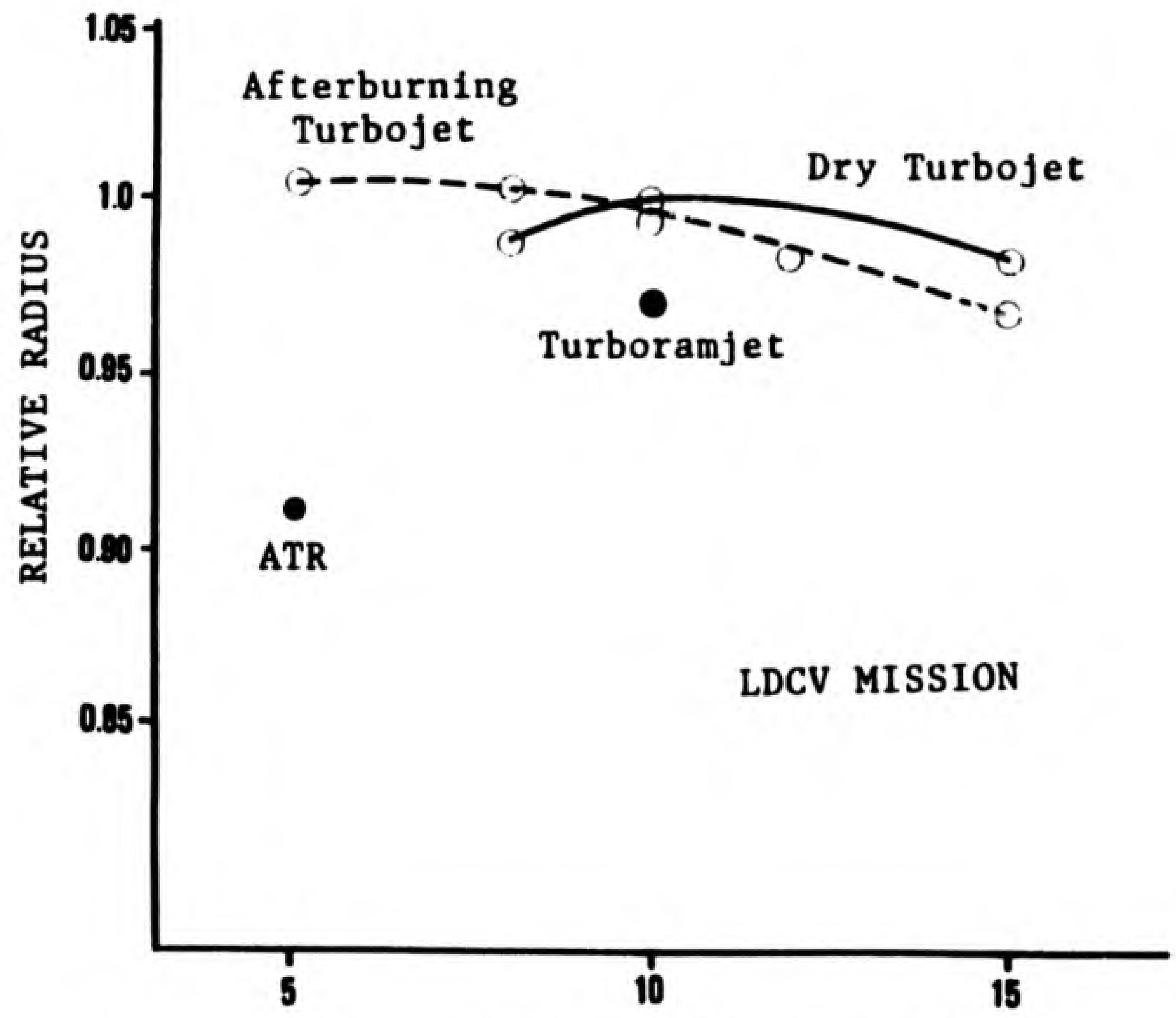

Figure 7 - Mission Performance Comparison

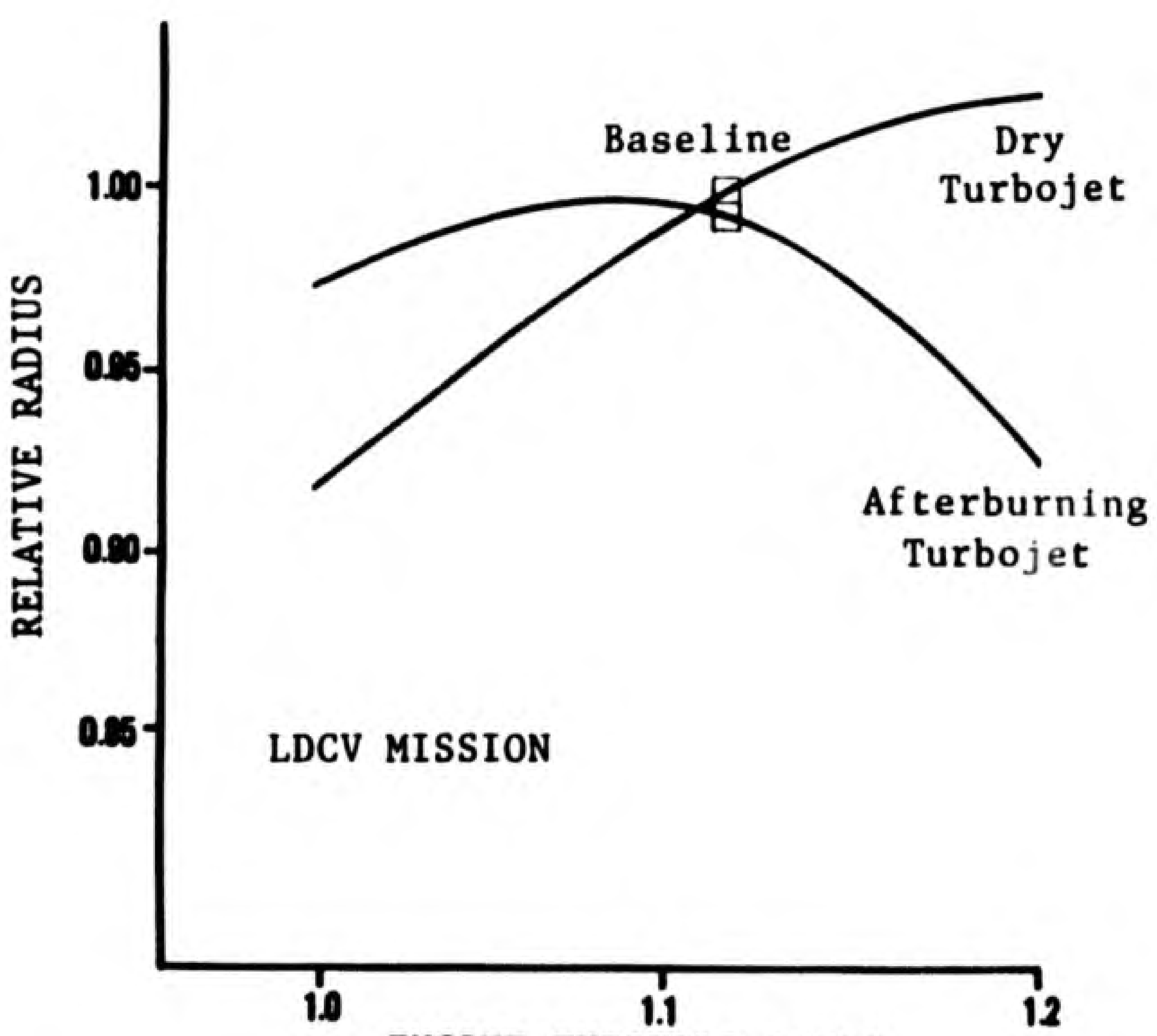

Figure 8 - Vehicle Sensitivity To Throttle Ratio

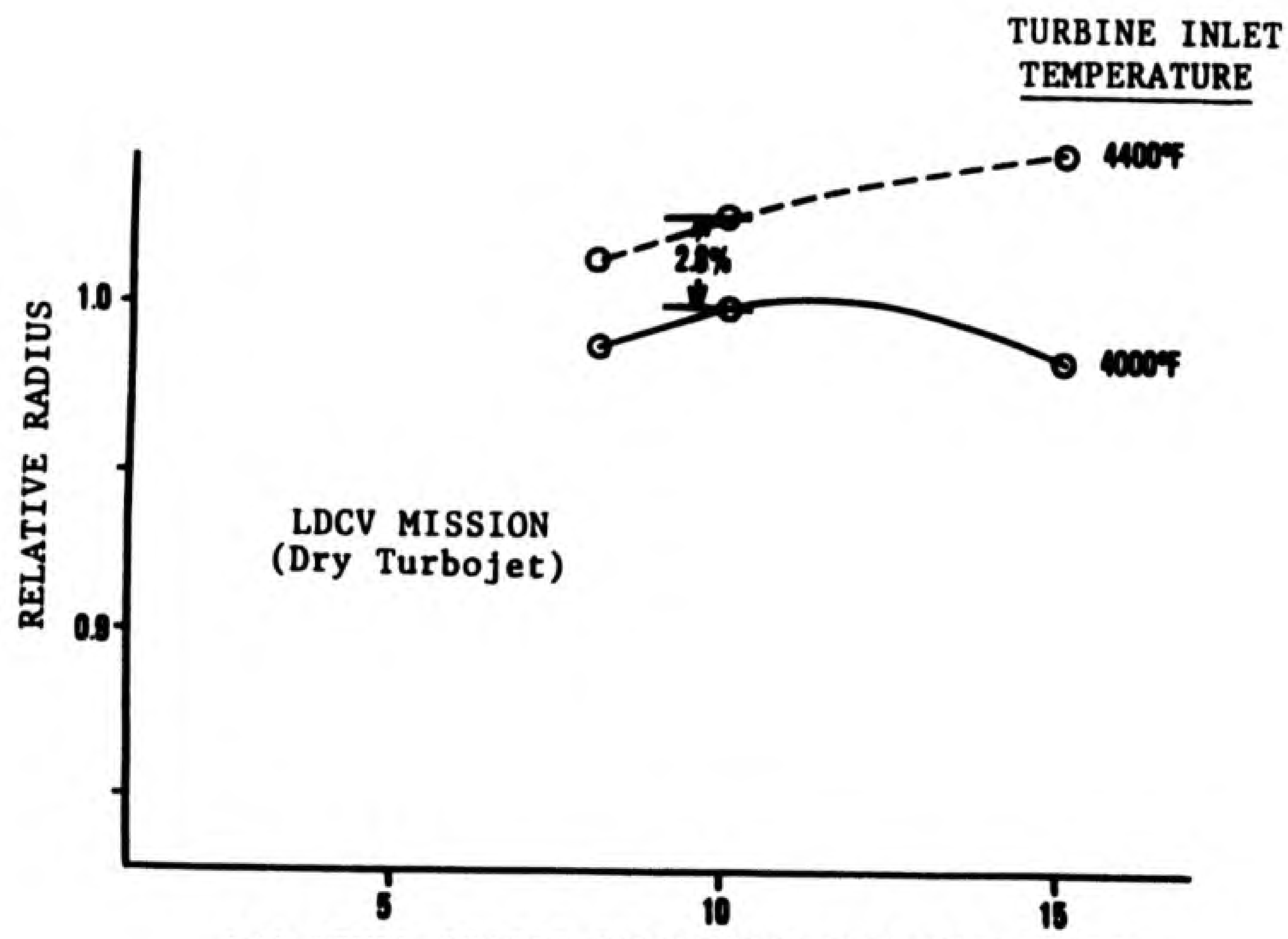

Figure 9 - Vehicle Sensitivity To Turbine Temperature

ratio to a higher value where the increased energy available can be better utilized. Assessments of SLS thrust-to-weight levels for both dry and afterburning turbojets indicated values of about 10 appear attractive. Radius benefits diminish rapidly at higher values.

As mentioned previously, future exhaust systems may not be able to fully expand the exhaust gasses at all flight speeds. One suggestion is to utilize the airframe aftbody as an expansion surface at maximum flight speeds. At transonic flight, additional base drag may result because of overexpansion on that aerodynamic surface. A sensitivity analysis was conducted to determine vehicle performance impact due to increased transonic drag. Installed transonic thrust was reduced 15%. Figure 10 illustrates how optimum compressor pressure ratio increases due to reduced transonic thrust. Also illustrated is the substantial influence of transonic engine performance on vehicle radius.

An effort was undertaken to assess the sensitivity of the mission radius to the engine/inlet matching. Airflow at Mach 5 for the dry and A/B turbojets was decreased by 15%. This led to a reduced inlet capture area and lower inlet bypass drag at transonic/low supersonic flight. Figure 11 reveals how the flow change improved mission performance for all but the high pressure ratio dry turbojets and shifted the optimum pressure ratio for both the dry and augmented designs to a lower value.

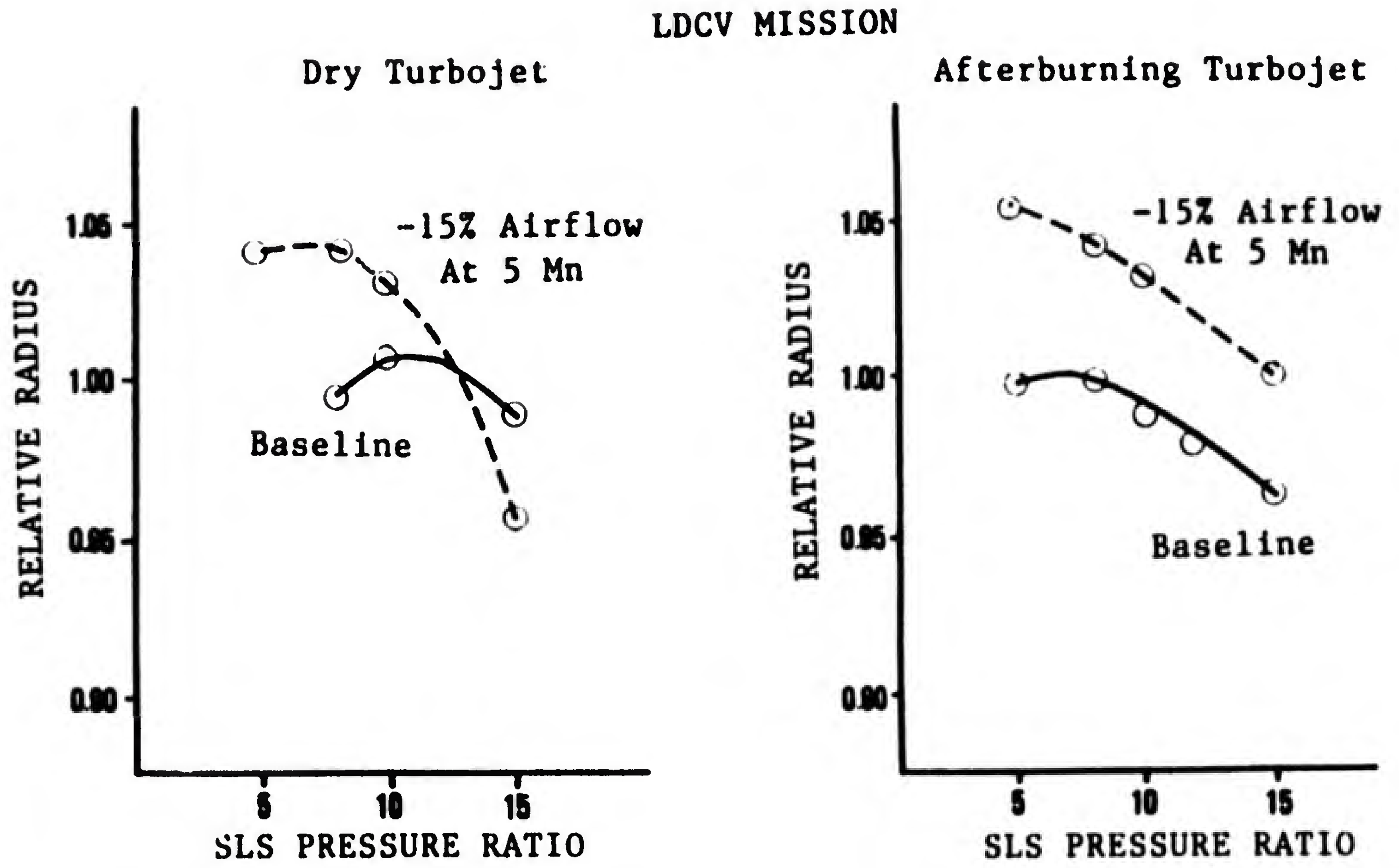

Figure 10 - Vehicle Sensitivity To Engine/Inlet Matching

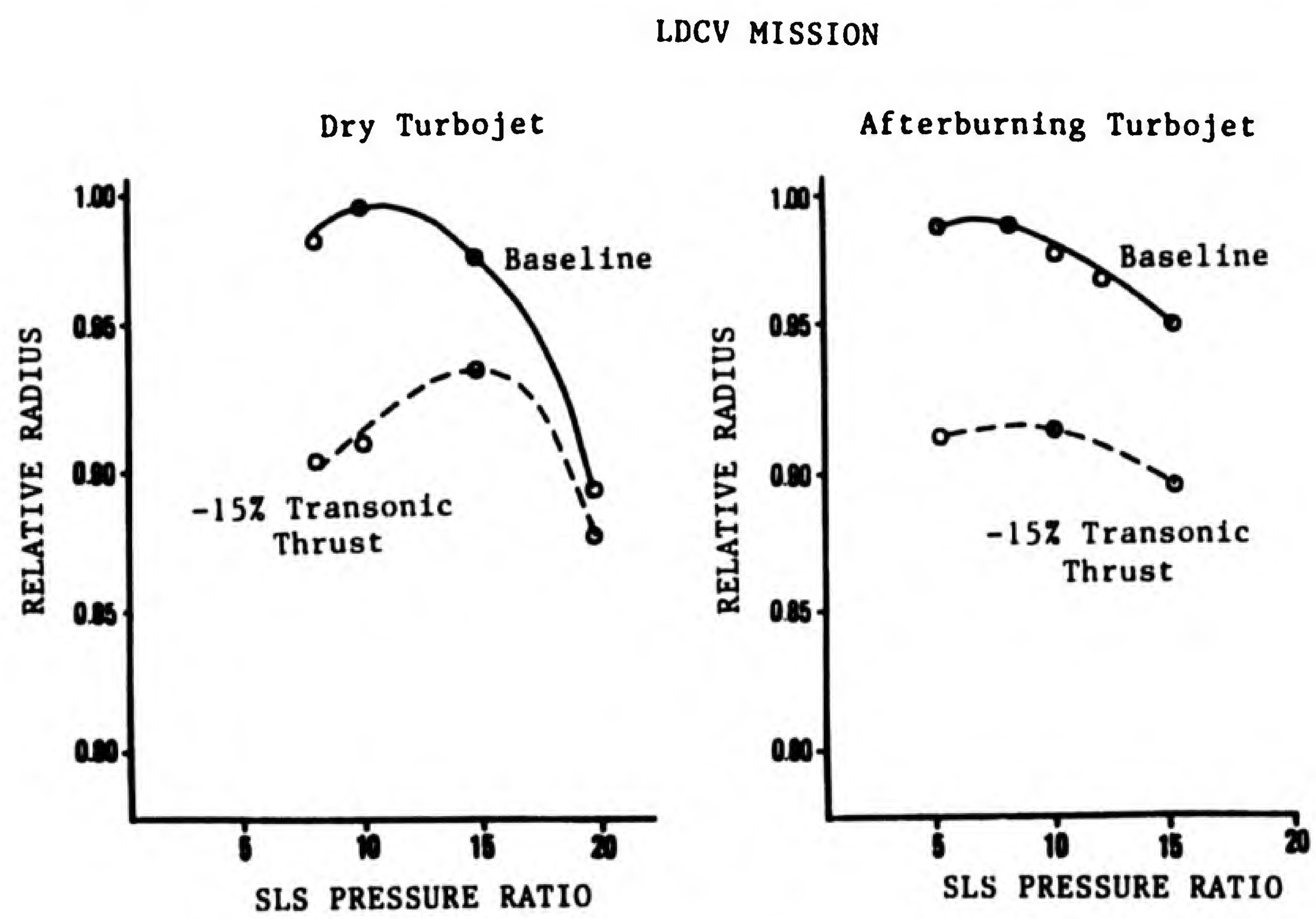

Figure 11 - Vehicle Sensitivity To Transonic Thrust

Short Duration High Acceleration Vehicle (SDHAV)

An alternate mission was examined which will be referred to in this paper as the Short Duration High Acceleration Vehicle (SDHAV). This mission utilized the same aircraft as described in Table 2. Conceived as a first stage accelerator, a maximum dynamic pressure (q) climb profile of 1000 pounds/square foot was assumed from sea level static until Mach 5 transition speed was obtained. Engine size is set by a requirement for time to accel/climb of 13.3 minutes (based upon related study efforts). Engine plus accel fuel weight became the figure of merit. Minimizing this weight combination allows more payload by reducing overall propulsion "dead weight".

Since the mission is essentially a max power run to speed, Mach 5 cruise fuel efficiency is not as critical as in the LDCV mission. This amplifies the effect of transonic thrust sizing. Figure 12 illustrates how the various engines compare along with the effect of pressure ratio. Again, turbine engine propulsion appears competitive. Optimum pressure ratios for the dry turbojet now occur at a lower value than for the afterburning configuration. This reversal from the LDCV mission is due to the lack of balance needed between cruise specific fuel consumption and thrust sizing requirements. Optimum pressure ratio for the dry turbojet occurs when minimum excess thrust is provided at both the transonic and Mach 5 operating condition. This results in lower propulsion weight due to engine size reductions which more than offset the increased acceleration fuel required. The afterburning engines optimize at a higher pressure ratio as compared to the previous mission because of the desire for high transonic specific thrust.

Mission performance variations due to engine characteristics exhibited the same

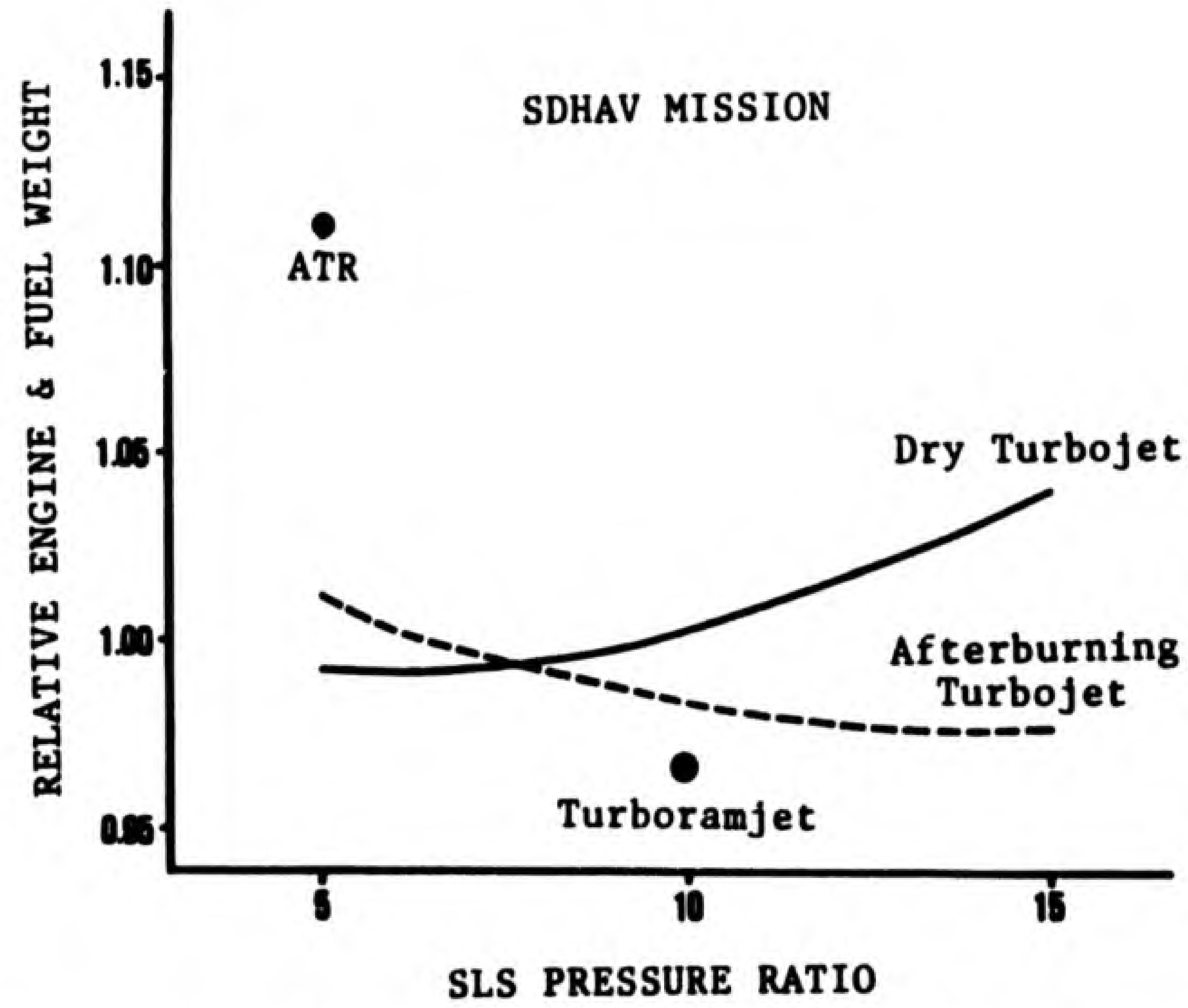

Figure 12 - Alternate Mission Performance Comparison

trends as described for the LDCV mission. Analysis of overexpansion at transonic flight speeds showed a moderate increase of optimum pressure ratio due to increased criticality of transonic thrust margin. For afterburning turbojets, reduced airflow at the inlet sizing point had a small effect on pressure ratio selection and tended to flatten out the performance curve. This is attributed to its thrust sizing point remaining at the transonic drag rise while reducing bypass and spillage drag. Conversely, a higher pressure ratio dry turbojet is thrust sized at maximum flight speeds which greatly increases the size and weight of the engines. Decreasing the flow size at this flight point amplified this condition.

Because of the special problems associated with turbine engines exposed to high speed flight, a conceptual study of various components including the compressor, turbine, combustor, heat exchanger, and nozzle was performed. The cycle selected for further analysis is described in Table 3. The conceptual design study encompassed a matrix of design variables and materials. The flight points used in the analysis are commensurate with a flight dynamic pressure of 1000 psf. For simplicity, only axial rotating stage configurations were considered.

AFTERBURNING TURBOJET (Sea Level Static, Standard Day)

Compressor Pressure Ratio	10
Max. Turbine Inlet Temp. (TIT)	2800°F
Afterburner Temperature	Stoichiometric
Throttle Ratio (TITmax/TITsls)	1.114
Component Adiabatic Efficiencies:	
Compressor	85%
Combustor	99%
Turbine	85%
Afterburner	95%
Pressure Losses:	
Combustor	9%
Exhaust Duct (dry)	1%
Cooling:	
Turbine Stator	0.0%
Turbine Rotor	0.0%
Exhaust Nozzle (Interstage Compressor Bleed)	15%
Fuel	Hydrogen
Nozzle Thrust Coefficient	.985

Table 3 - Baseline Engine Cycle Stack

Compressor

At Mach 5 flight, the compressor exit temperature presented in Figure 13 allows for three potential materials: Columbium, ceramic composite, and carbon-carbon. It is the opinion of the authors that carbon-carbon (c/c) represents the highest risk and columbium the lowest. To simplify the design matrix, each compressor was assumed to be monolithic (made of one material). Columbium blading was assumed to be uncoated. With this assumption, design constraints for columbium were considered to be equivalent to current metallic blading technology development. Ceramic composites and carbon-carbon were set at lower levels due to their structural limitations and coating requirements. Columbium first stage aerodynamic loading was limited to a level commensurate with advanced nickel alloy compressors. In this paper, aerodynamic loading is defined as:

$$\text{Aerodynamic loading} = \frac{g(J)(\Delta H)}{Uh^2}$$

Where:

g = 32.2 ft/sec
J = 778 ft-lbs/BTU
ΔH = Delta enthalpy (BTU/lbm)
Uh = Hub speed (ft/sec)

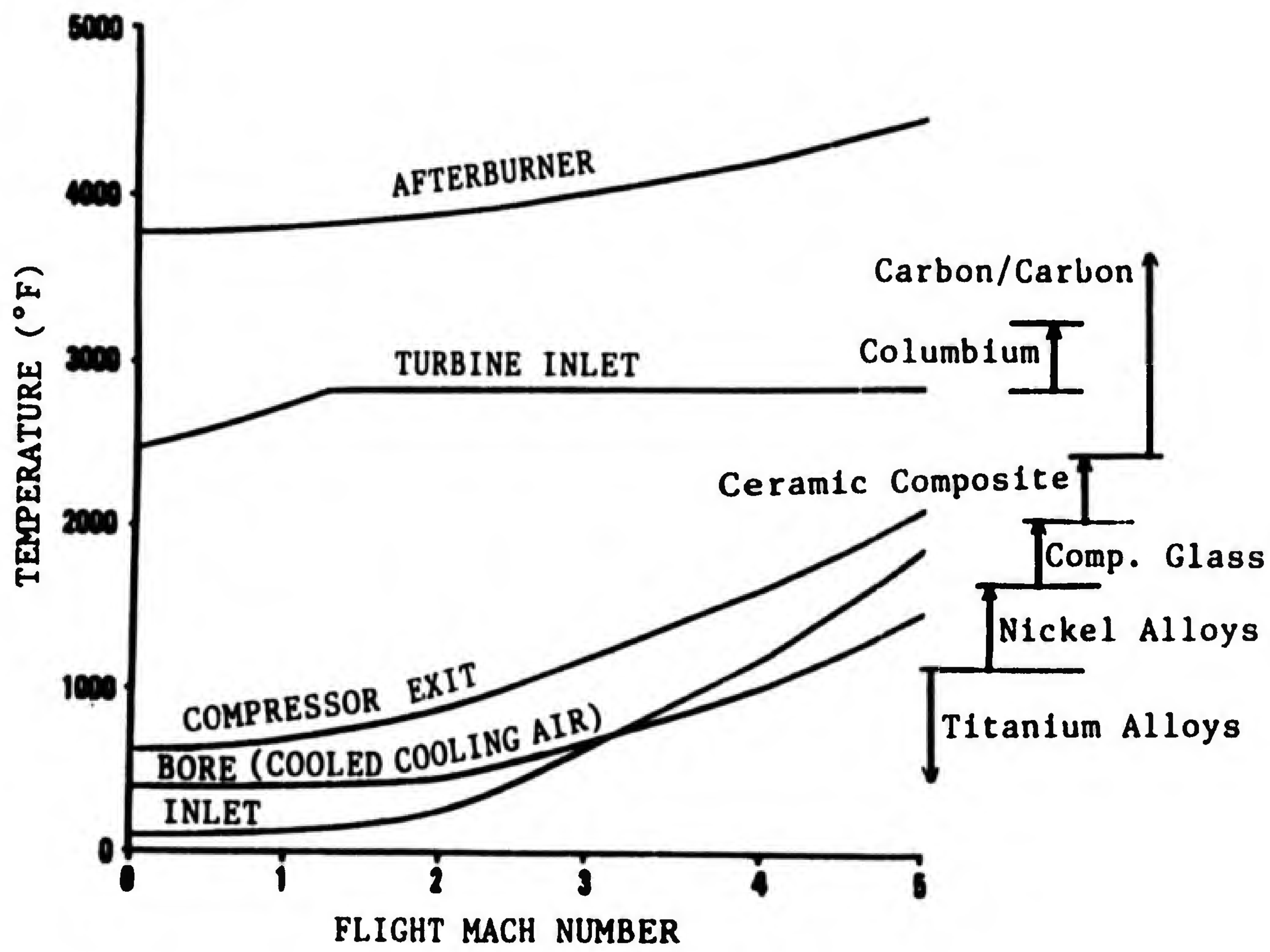

Figure 13 - Mach No. Impact On Component Gas Temperatures

Structural and mechanical limitations for the non-metallic materials are anticipated to restrict the blade camber and twist. Therefore, the aerodynamic loading for carbon-carbon was reduced 50% relative to columbium while the ceramic composite was fixed near the median between the two. For all compressor designs, a constant tip diameter design was chosen for simplicity and enhanced aerodynamic loading. To maximize the potential performance, each compressor configuration was assumed to be designed at its maximum loading. Figure 14 shows the tip relative Mach numbers for each material. Ceramic composites and carbon-carbon, because of structural and coating considerations, need large leading edge radii resulting in excessive shock losses at higher inlet relative Mach numbers. Hence, these materials cannot run at the inlet relative Mach number levels of the uncoated columbium.

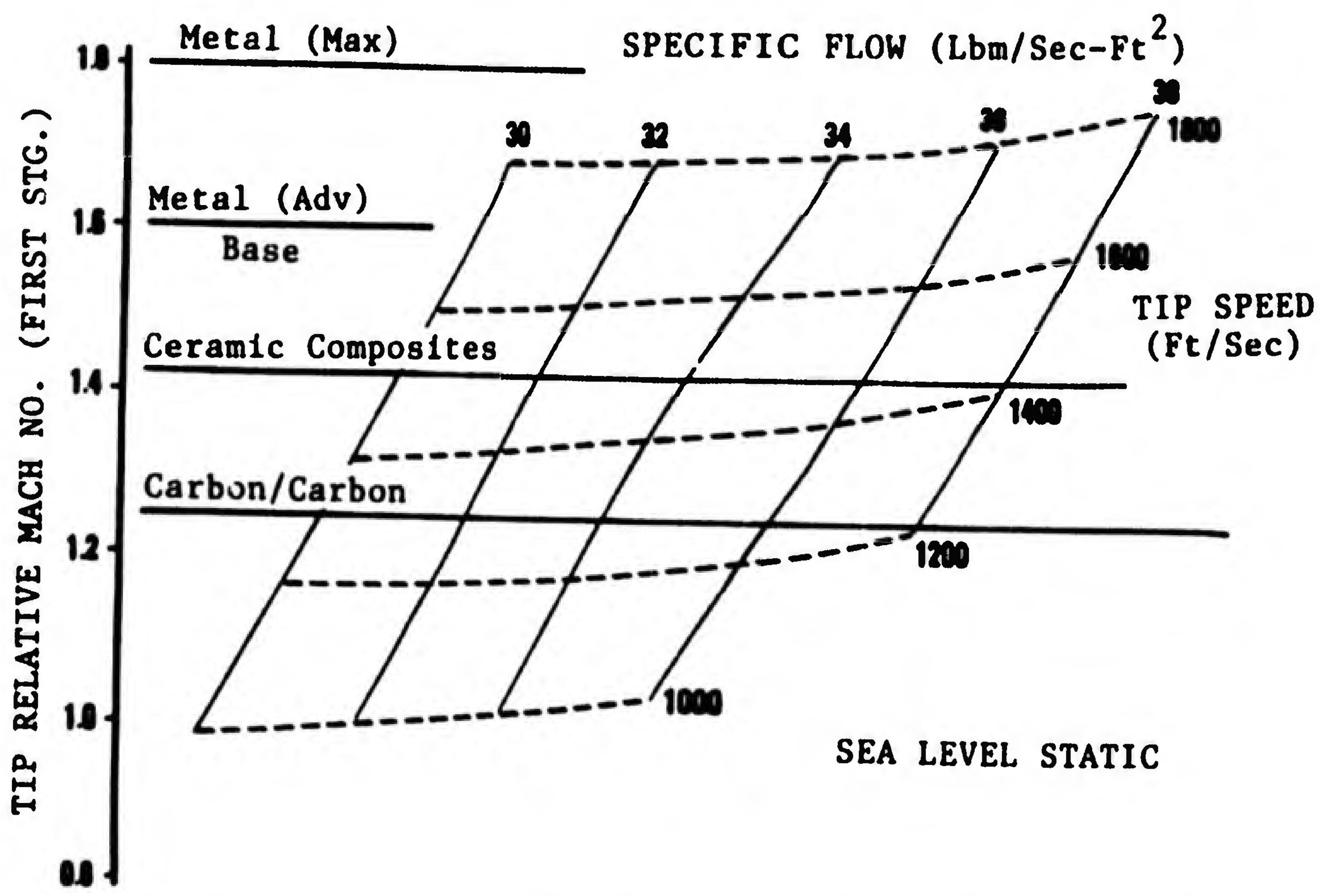

Figure 14 - Compressor Tip Relative Mach No. Comparison

With compressor size and speed determined by the inlet design, compressor exit size was found. Sea level static, maximum power was used as the design point based on an assessment of the variation of compressor exit axial Mach number along the flight path. Compressor exit axial Mach number was set at 0.35 at design to satisfy diffuser and combustor requirements. Several variations of design pressure ratio and stage count were assessed. For this paper, only the baseline cycle will be presented.

Figure 15 shows compressor frontal area as a function of radius ratio. The inlet radius ratio of each material design is set by a desire for minimum compressor frontal area. Decreasing the stage count leads to increased stage work which requires increased blade speed and radius ratio to stay within design limits. For both carbon-carbon and ceramic composite compressors, increasing the number of stages beyond six appears to have diminishing returns when qualitatively evaluated against the added weight of extra stages as well as the structural implications of the low radius ratio design. For the columbium compressor, it was determined that the minimum number of compressor stages is three, in order to meet design requirements.

Figure 16 shows the baseline compressor designs for all three materials. Additional benefits of higher loading capability are exhibited by the significant frontal area reduction for the columbium and ceramic composite compressors relative to carbon-carbon. Figure 17 illustrates how the exit rim speeds of the three compressors compare to current man-rated designs as a function of compressor exit temperature. Shown is that all three designs require revolutionary advancements. Some reduction in engine life requirements would help to reduce this significant technology jump.

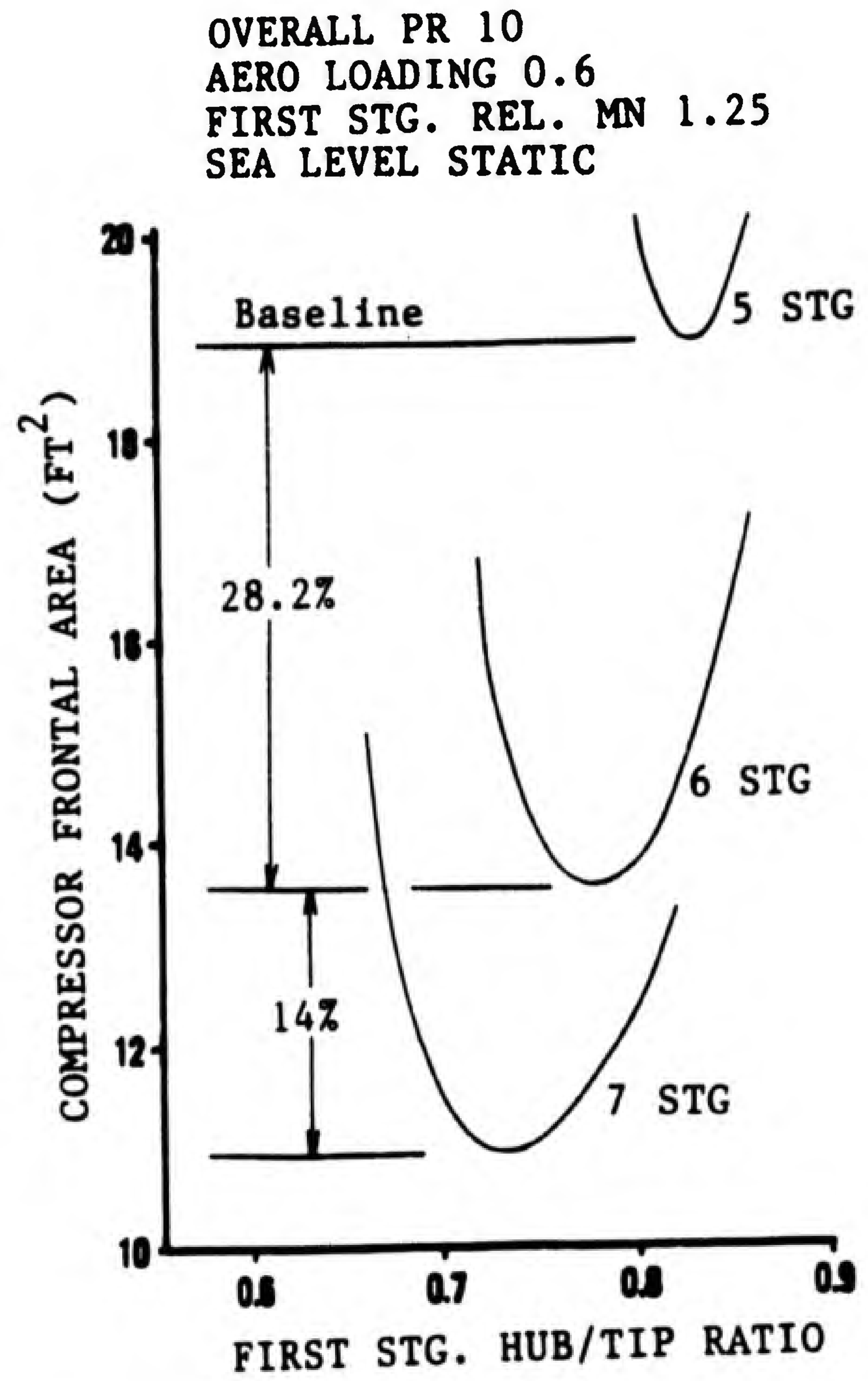

Figure 15 - Compressor Stage No. Impact On Frontal Area

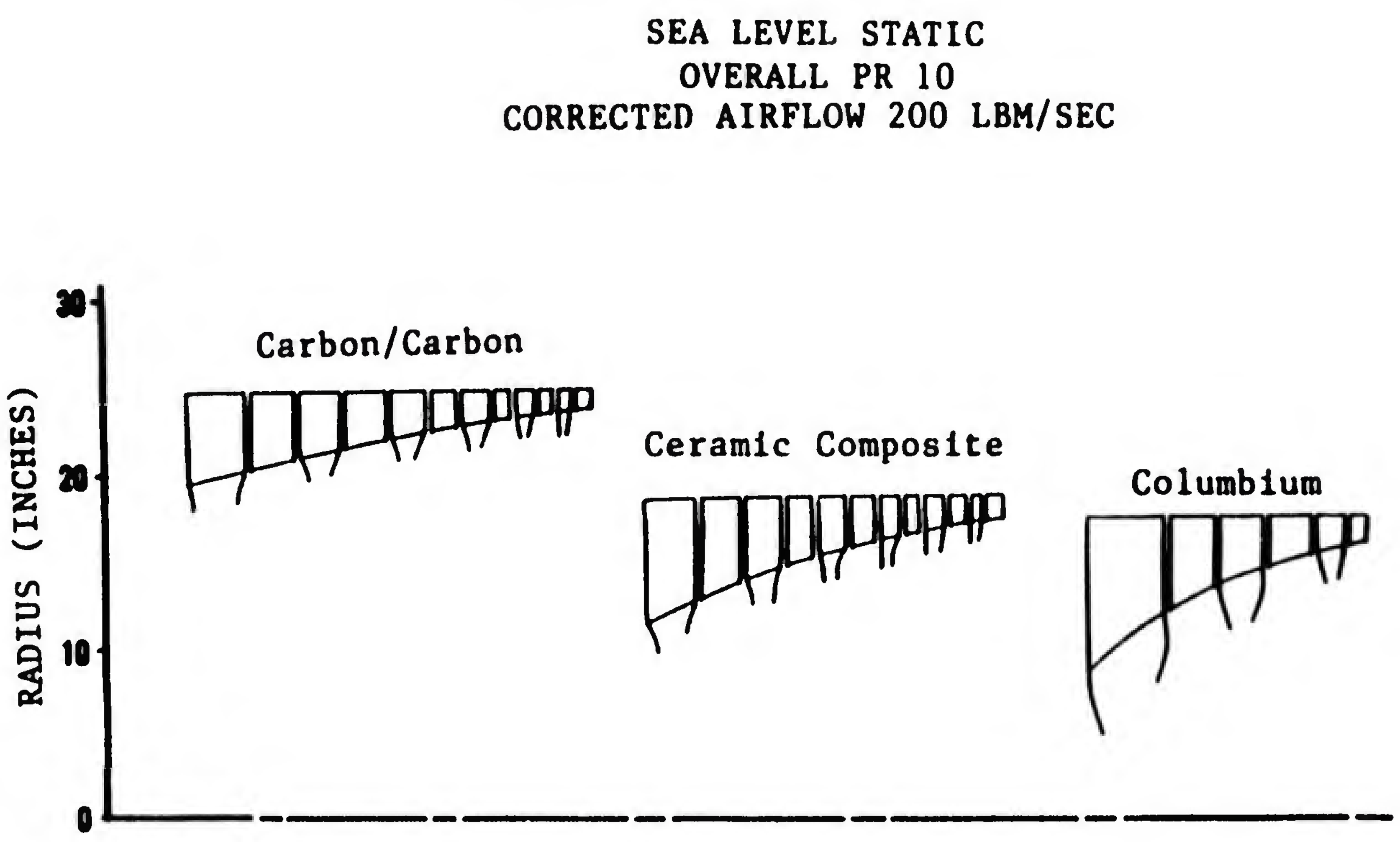

Figure 16 - Compressor Layout Options

TURBINE

Figure 13 shows that for the uncooled turbine inlet temperature selected, only columbium and carbon-carbon are viable material candidates for an uncooled turbine. Figure 18 compares the baseline afterburning turbojet with and without turbine cooling at two flight conditions. The cooled turbine assumes 5% of the engine airflow is used for turbine cooling. Shown is that turbine cooling has little effect on overall engine performance. Therefore, a material with marginal temperature capability could be used with some degree of turbine cooling. Ceramic composite turbines were evaluated with the assumption that the turbine would be high risk in an uncooled configuration and moderate risk in a cooled configuration.

Evaluating the turbine design at its flow sizing condition, Figure 19 shows how the rim radius varies as a function of stage number and aerodynamic loading. Aerodynamic loading is defined in the same manner as specified for the compressor. The turbine was assumed to be a constant rim radius to enhance its energy extraction potential. As the stage aerodynamic load increases, the rim radius decreases yielding a more streamlined flowpath design, reducing frontal area and weight as well as turbine rim speed. Assuming a choked turbine inlet, a nominal flowpath divergence, and a representative exit Mach number, Figure 20 shows how the turbine flowpath varies relative to the three baseline compressors for one, two and three stage turbines at these aerodynamic loadings. The desire to minimize both frontal area and number of stages is most easily achieved with the columbium turbine which requires only a single stage turbine. For the non-metallics, two stage designs appear most attractive at these loading levels. Higher loading levels

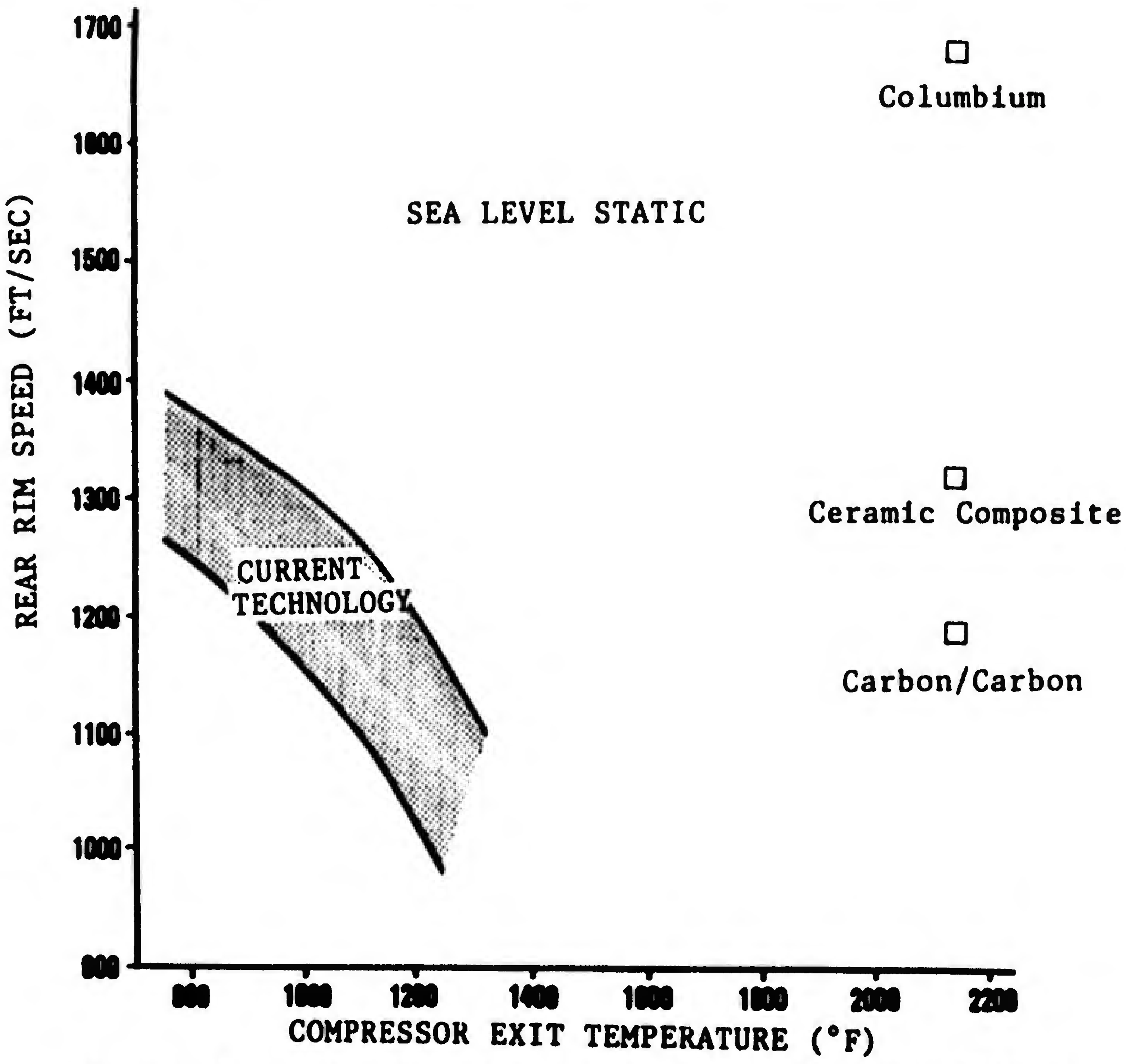

Figure 17 - High Mach Compressor Material Requirements

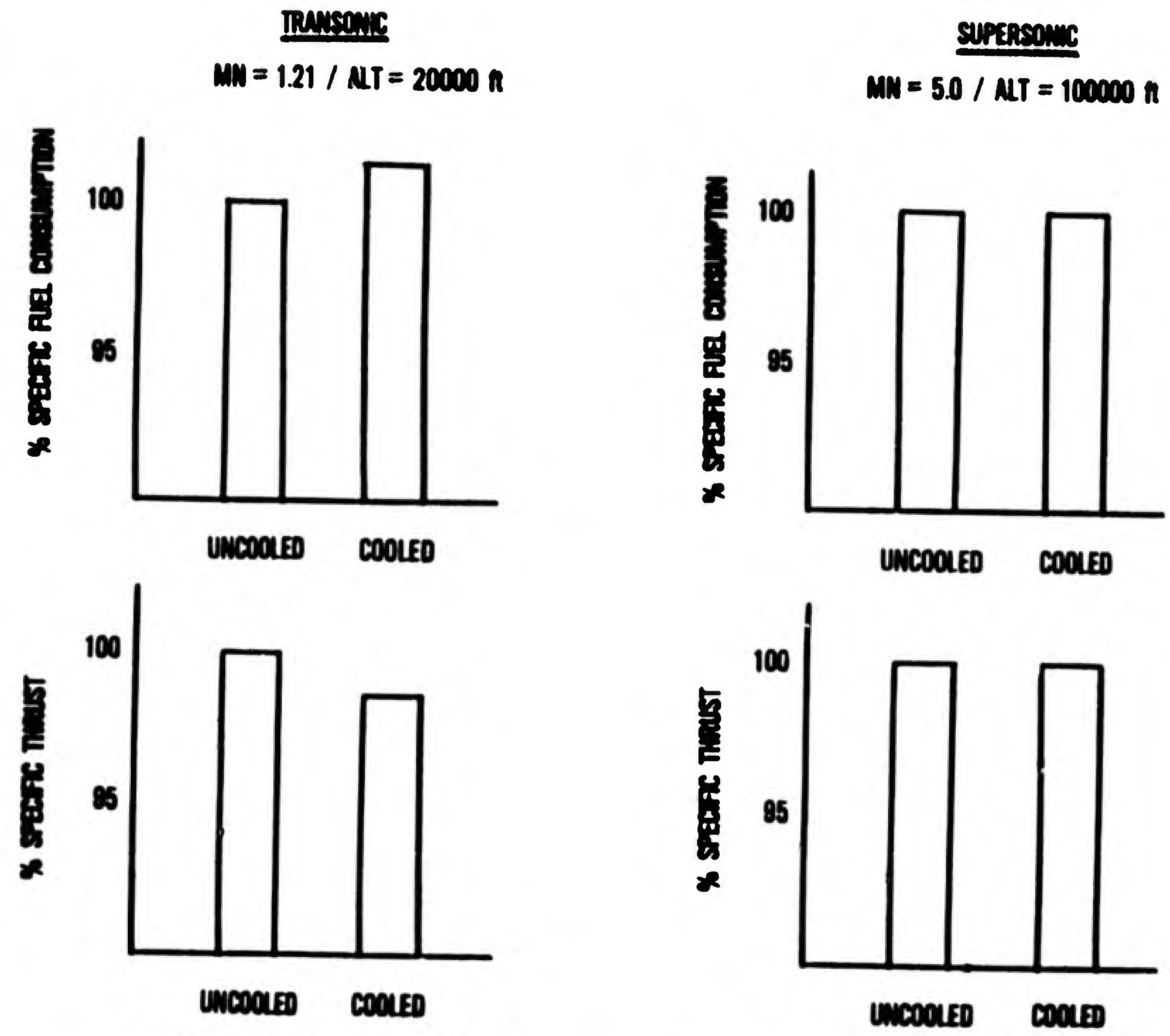

Figure 18 - Turbine Cooling Impact On Performance

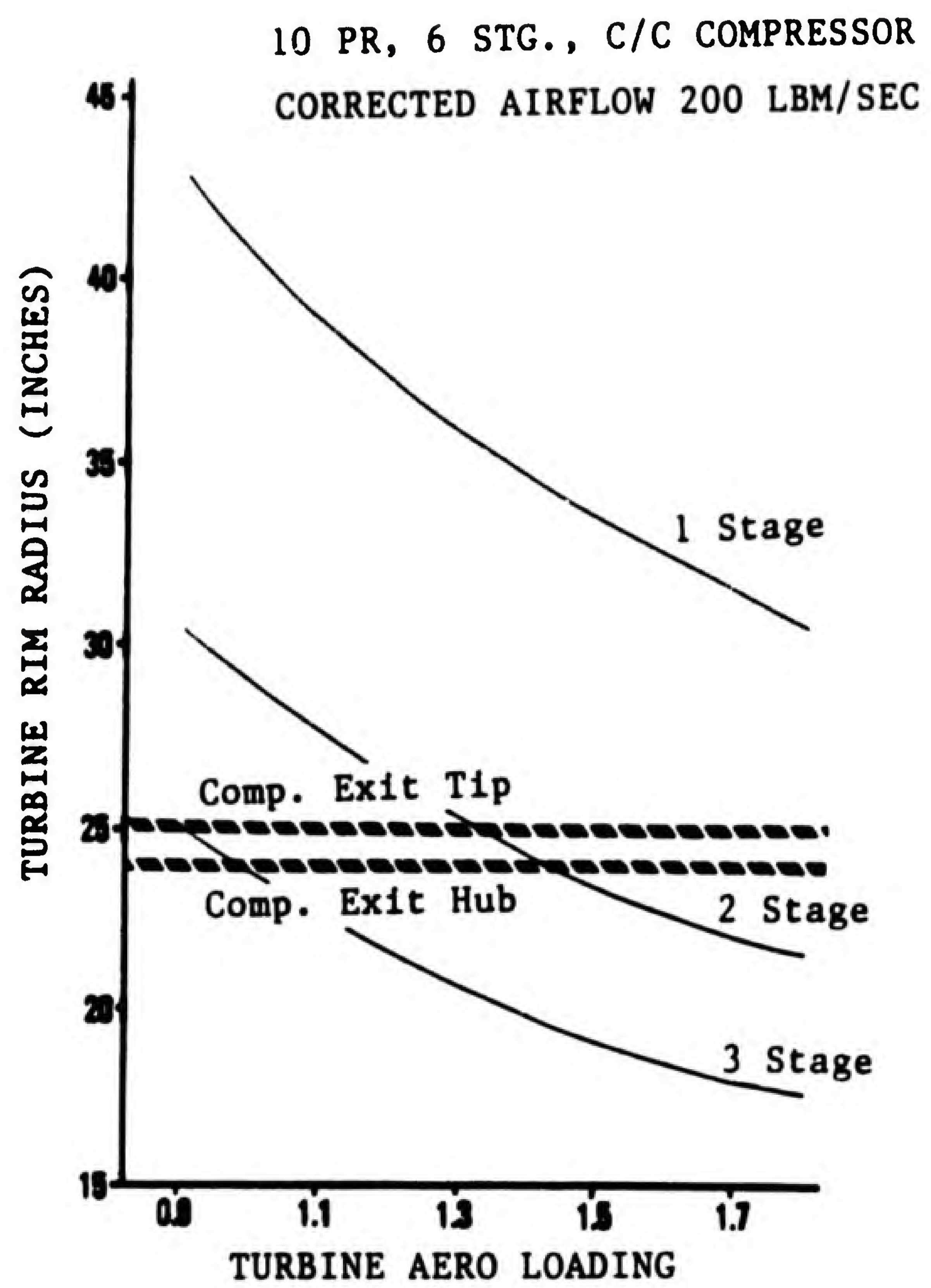

Figure 19 - Turbine Design Tradeoffs

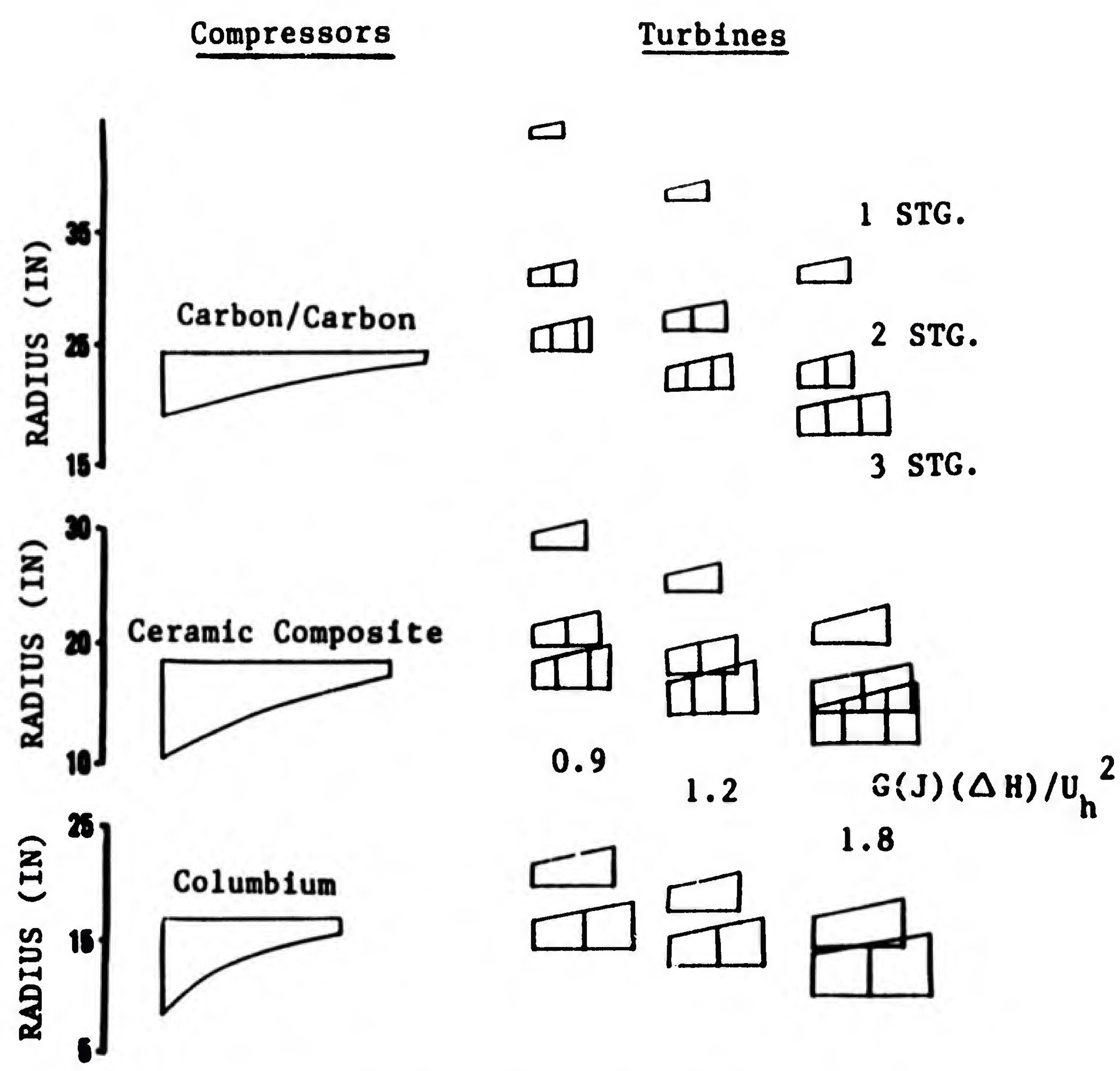

Figure 20 - Turbine Design Matrix

may be possible which result in a single stage turbine design. A single stage, non-metallic design presents higher structural and manufacturing risks.

Figure 21 shows the corrected work required as a function of flight Mach number. Corrected work is defined as:

$$W_{corr} = \frac{\Delta H}{\theta}$$

Where:
ΔH = Delta enthalpy
θ = Turbine Inlet Temperature (deg R)/519.

Compared to current metallic turbines, work levels are well within the state-of-the-art for single stage designs. For non-metallics, the risk is considered moderate for the two stage designs. Two stage turbines were chosen for the non-metallic baseline designs while the metallic turbine utilized one stage.

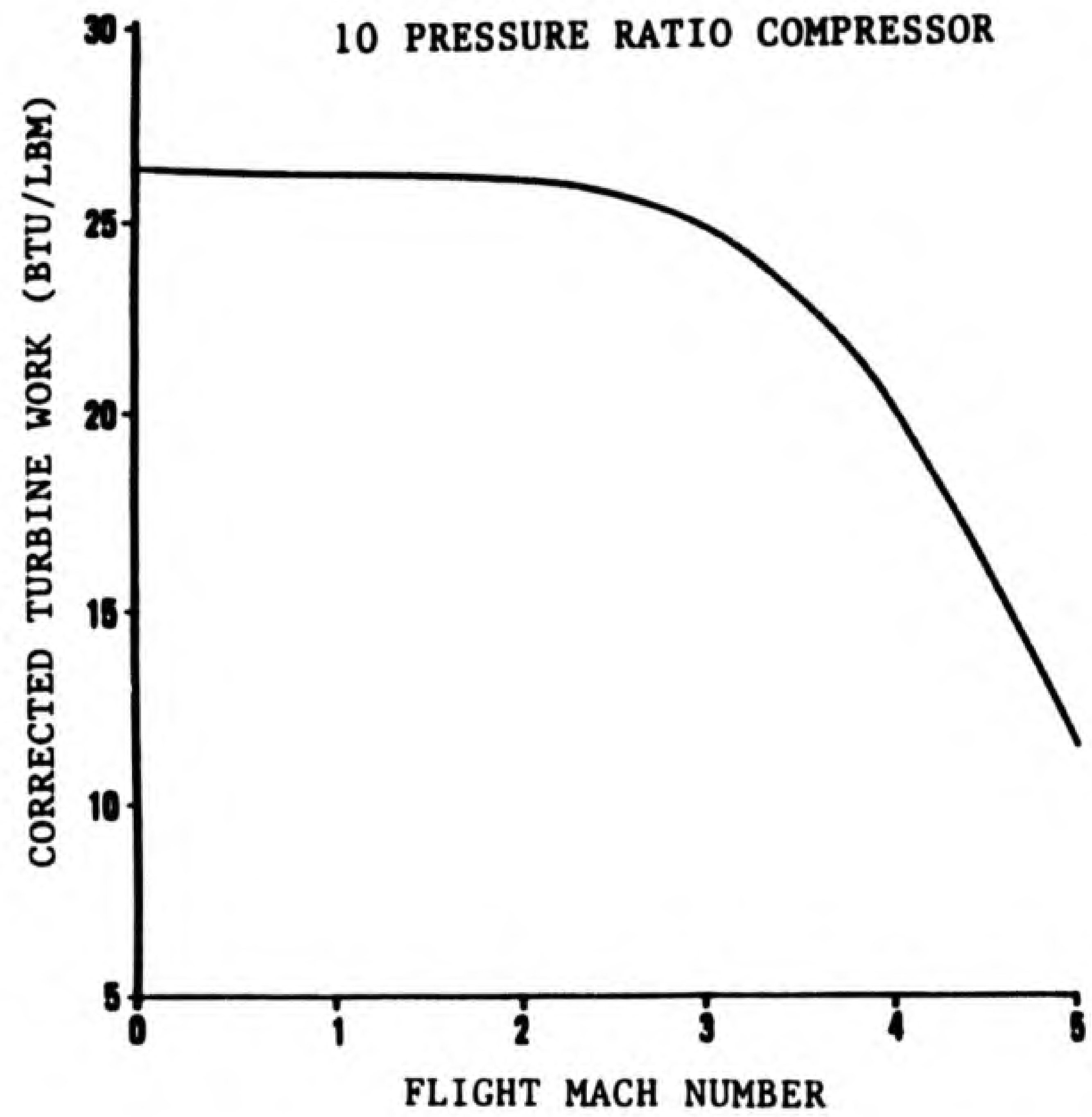

Figure 21 - Turbine Work Requirements

COMBUSTOR

The combustor geometry was defined by centering the inner and outer radii about the turbine inlet. Using the results of the engine cycle analysis and assumed values of combustor length to height, the combustor volume, space heat rate and burner residence time were calculated. Combustor sizing and heat release loadings were evaluated across the flight path.

Figure 22 shows the interrelationship between various combustor design parameters. Space heat rate increases rapidly with increasing combustor reference velocity. It was assumed that using hydrogen fuel would allow higher than typical space heat rates currently used for JP type fuels. A maximum space heat rate value of 20 million btu/hr-ft-atm was chosen resulting in a burner residence time of 4.6 milliseconds.

Indications are that with some development risk, the hydrogen combustor is feasible. The greatest challenge to the combustor design is projected to be in the fuel delivery system because of the high fuel inlet temperatures.

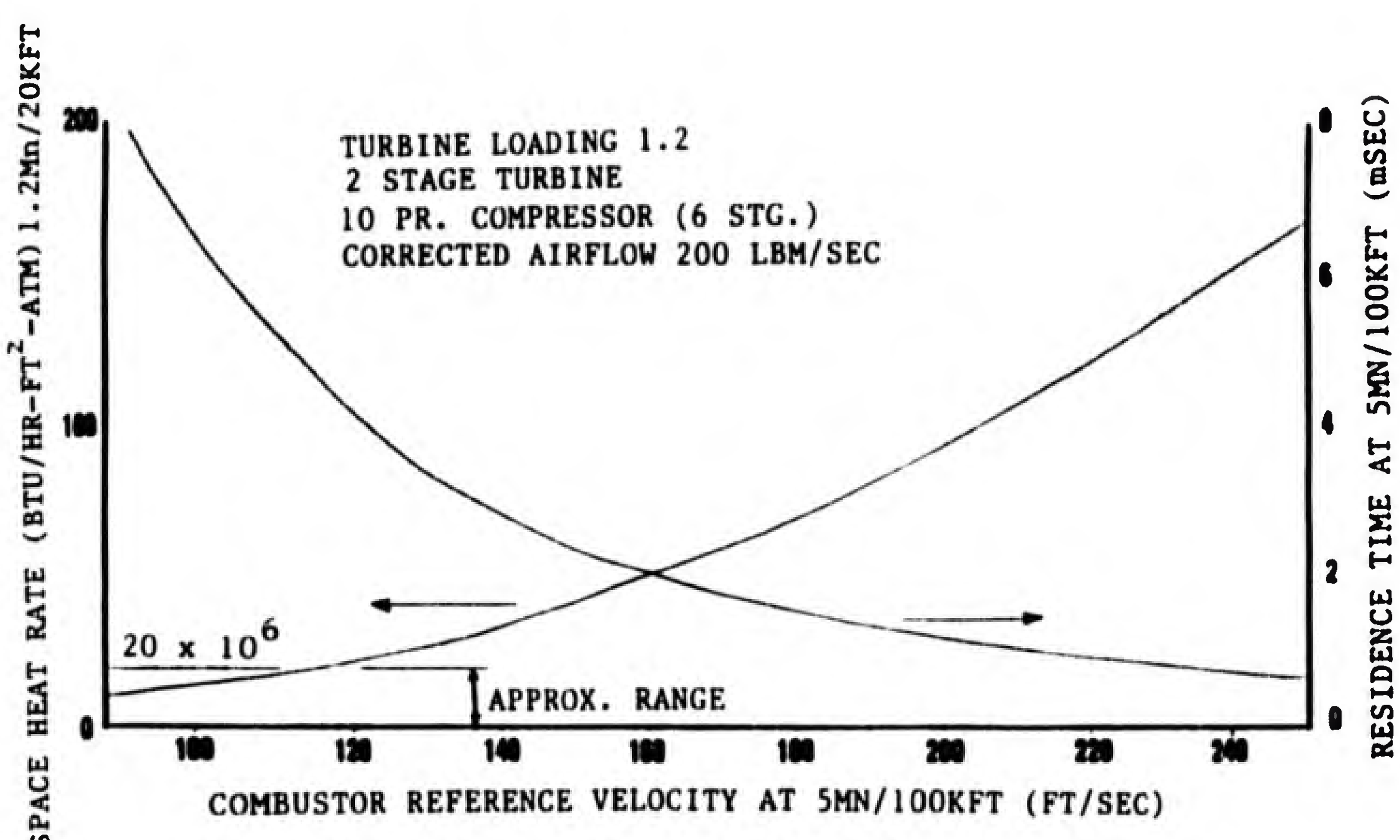

Figure 22 - Combustor Design Tradeoffs

HEAT EXCHANGERS

One of the more critical technologies for hypersonic flight will be the distribution and control of thermal loads. Figure 13 shows that even inlet air temperatures at Mach 5 are too high for cooling the nozzle and bore components. Using the heat sink capability of the hydrogen fuel, a fuel/air heat exchanger was used to cool engine air for critical system components at all flight speeds above Mach 4. The hydrogen fuel temperature entering the heat exchanger was elevated from its tank temperature to simulate aircraft cooling requirements.

Figure 23 shows the variation in combustor inlet fuel and cooling air temperature as a function of compressor exit bleed air and aircraft fuel delivery temperature. The shaded areas indicated regions of interest for various flight speeds. At Mach 5, the cooling air temperature is reduced 15% from compressor discharge temperature. Heat exchanger fuel inlet temperature was fixed at 800°F based upon estimated aircraft heat load requirements.

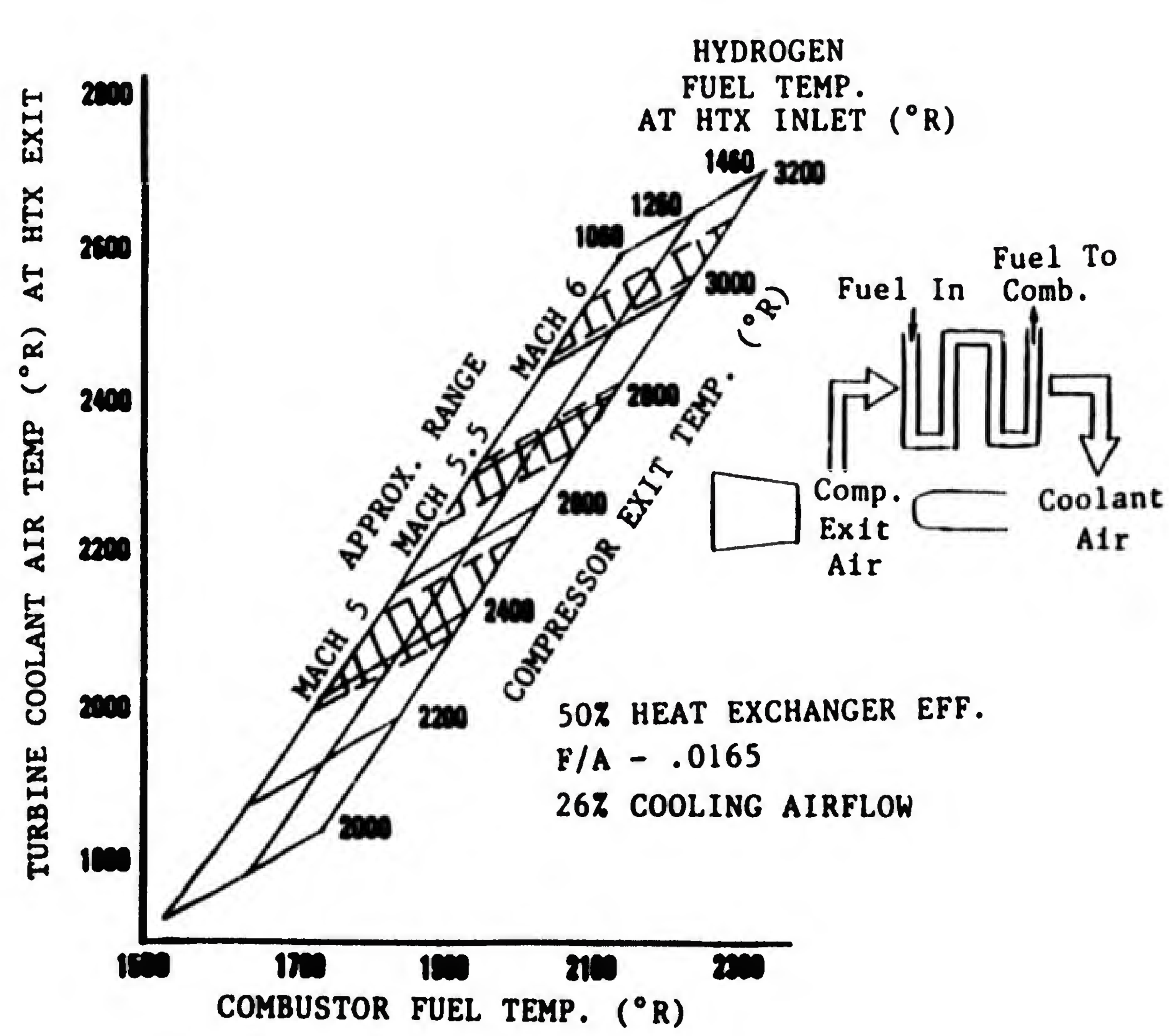

Figure 23 - Heat Exchanger (HTX) Temperature Tradeoffs

The engine bore will require further cooling than previously described. Suggested is that a portion of fuel be tapped prior to full aircraft routing and used to cool a small portion of compressor bleed air. Due to the small amount of flow required, this heat exchanger could conceivably be integrated into the bore area. With this approach, it is believed that the bore components may be cooled sufficiently for reasonable life retention. The high risk associated with this technology can be reduced by the introduction of advanced high temperature bore components (i.e. bearings, seals, etc.) and innovative structural/mechanical designs.

EXHAUST NOZZLE

The exhaust nozzle represents the most critical technology for superior aircraft performance. Nozzle internal thrust performance must be balanced across the flight envelope with installation effects such as boat tail and wave drag. For this conceptual design, a simplistic approach was used with only internal performance considered using the loss stack-up shown in Figure 24. This figure illustrates the trade between expansion and angularity losses as a function of area ratio. A nozzle length to diameter ratio of 7 was assumed. Peak performance occurs between 15 and 16 area ratio. However, because of diminishing returns, an area ratio of 10 was considered in addition to a fully expanded design.

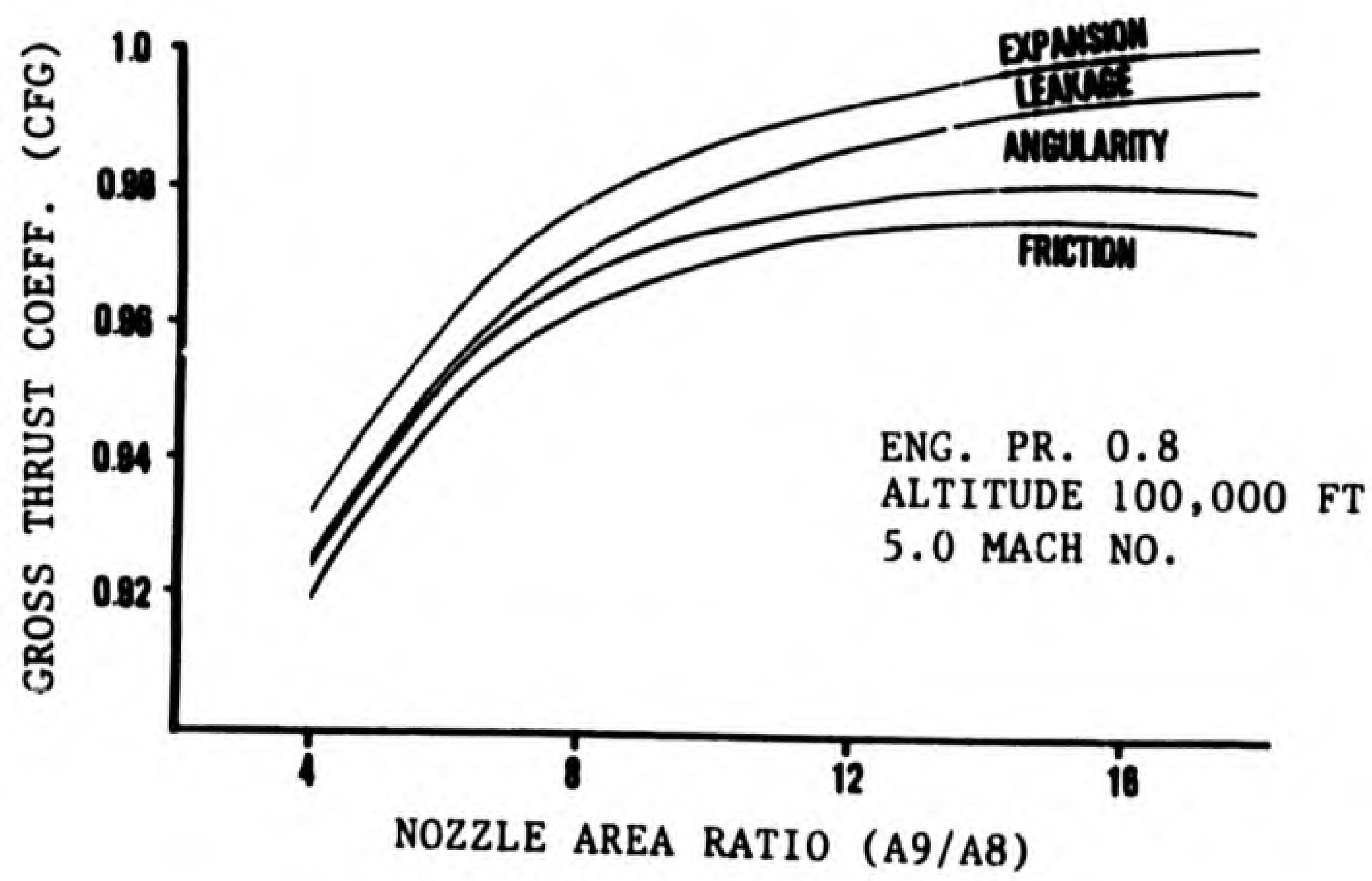

Figure 24 - Nozzle Loss Buildup

Figure 25 compares the full expansion nozzle, the 10 area ratio nozzle using straight flaps, and the 10 area ratio design using a bell curvature design for the diverging flap. The full expansion nozzle thrust coefficient is approximately 98.3% and is over 5.5 feet longer than the baseline area ratio nozzle which incorporated a thrust coefficient of 96.9%. The bell shaped nozzle is projected to have equivalent performance as the straight flapped version but with a reduced length of almost 4 feet. For reasons of reduced weight, the 10 area ratio, bell shaped nozzle was chosen.

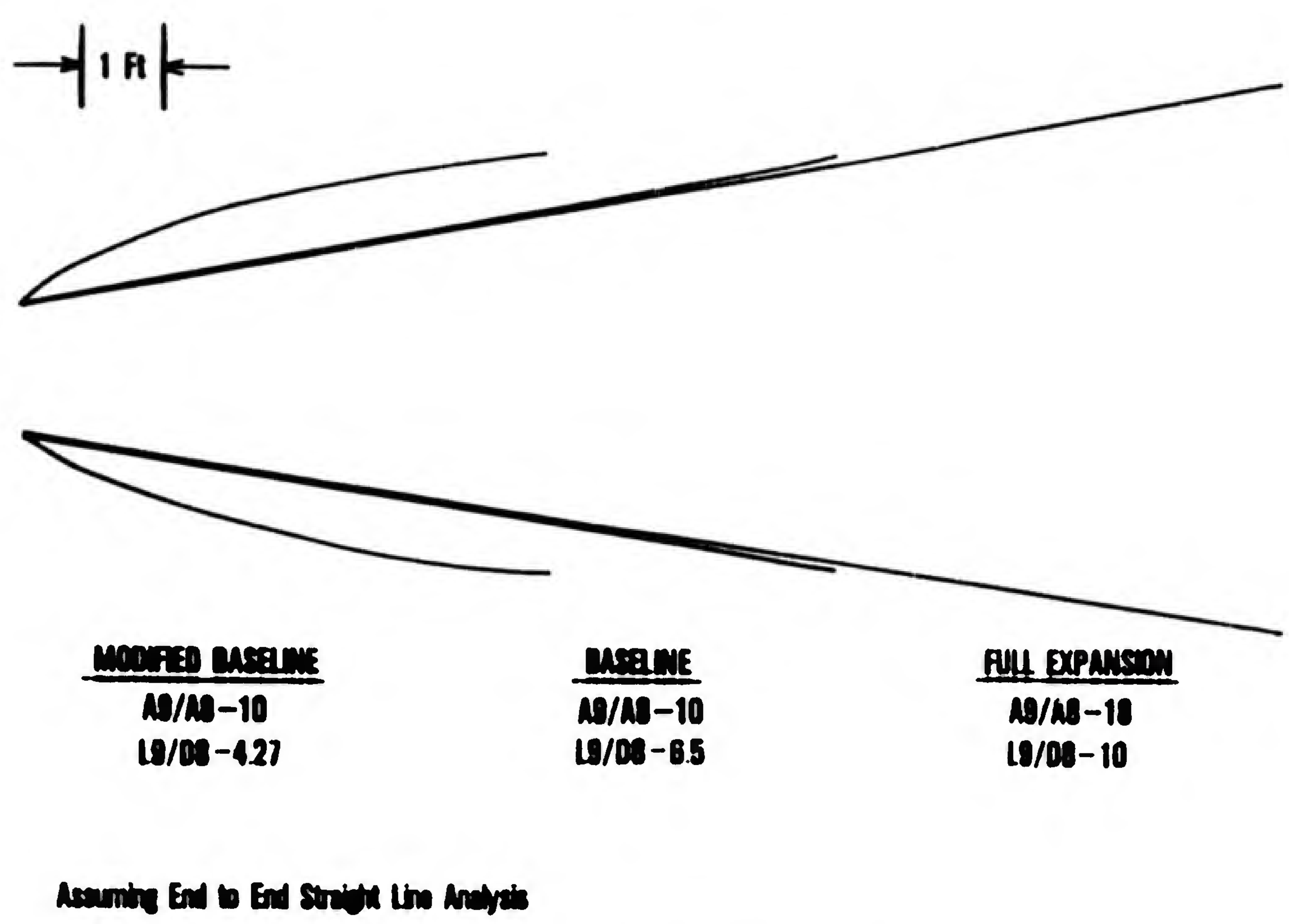

Figure 25 - Nozzle Design Options

CONCLUSIONS/RECOMMENDATIONS

The performance analysis presented indicates that the turbine engine provides competitive performance up to low hypersonic flight velocities. Described have been the desirable operating characteristics, both uninstalled and installed. Sensitivity analyses at Mach 5 indicate that nozzle gross thrust coefficient is of prime importance, with component efficiencies having a secondary impact on performance. The dry turbojet requires very high levels of turbine inlet temperature to have competitive specific thrust. For all cycles, proper engine/inlet flow matching can substantially enhance vehicle performance. From a technology risk standpoint, the afterburning turbojet is more desirable. It does not require the very high levels of turbine inlet temperature as dictated for the dry turbojet cycle and provides competitive performance to the turboramjet with substantially reduced complexity.

Key components needed for an afterburning turbojet for Mach 5 operation have been assessed to determine their feasibility. From a conceptual design standpoint, there appears to be no technology barriers which preclude the development of this system. There are however, various levels of risk associated with the different components which can only be overcome by exploratory and advanced development efforts. It is recommended that research programs be formulated to address these technology challenges. It is further recommended that the turbomachinery concept be considered in future activities relating to hypersonic propulsion devices because of the tremendous potential payoffs in terms of simplicity and performance.

ACKNOWLEDGMENT

The authors wish to thank Mr. Errol G. Blevins for his computer support and Messrs. Christopher M. Norden and Walter D. Hoy for their substantial assistance in generating data in all phases of this study. It is through their support that this study could be successfully completed.

REFERENCES

1. APL TDR 64-61, "Inlet Efficiency Parameters for Supersonic Combustion Ramjet Engines," E. T. Curran, Sqn Ldr, RAF, M. B. Bergsten, June, 1964.

2. NASA-CR-158926-Vol 2, "Hypersonic Cruise Aircraft Propulsion Integration Study," 1979 (Lockheed-California Co., Burbank).

Discussion

RAMETTE

For the carbon/carbon compressor, did you take into account the oxydation problem, the protective coating which is needed and the correlative impact on the air flow.

AUTHOR'S REPLY

Yes; the carbon/carbon and ceramic composite compressors were assumed to be coated. The result is a reduced aerodynamic loading and increased leading edge radius for these materials. This is why the carbon/carbon and ceramic composite compressor are larger in radius and require more stages to produce the pressure ratio of 10 at sea level static.

BOURY

Do you think that such an advanced turbojet could be a good accelerator for the NASP?

AUTHOR'S REPLY

Yes, I do. This in no way implies that this configuration is or is not currently under consideration. This study was performed totally outside the realm of NASP.

RODI

What kind of materials do you envisage for bearings and what kind of fluids for cooling and lubrication systems?

AUTHOR'S REPLY

I cannot comment on this question.

TARIFA

1. Would you explain the cooling system of your nozzles and the fig of 15% cooling flow.
2. Have you considered the possibility of the use of other nozzles as plug nozzles with advanced materials?

AUTHOR'S REPLY

1. We feel that 15% would be adequate to cool the various components.
2. No, we did not.